Article:
Ritzefeld, M, Wright, MH orcid.org/0000-0003-2731-4707 and Tate, EW (2018) New developments in probing and targeting protein acylation in malaria, leishmaniasis and African sleeping sickness. Parasitology, 145 (2). pp. 157-174. ISSN 0031-1820

https://doi.org/10.1017/S0031182017000282

New developments in probing and targeting protein acylation in malaria, leishmaniasis and African sleeping sickness

Markus Ritzefeld[1,a], Megan H. Wright[2,a] and Edward W. Tate[1,*]

[1] Department of Chemistry, Imperial College London, SW7 2AZ, UK

[2] School of Chemistry, University of Leeds, LS2 9JT, UK

*Corresponding author: +44 (0)20 7594 3752. E-mail: e.tate@imperial.ac.uk

[a]These authors contributed equally.

SUMMARY

Infections by protozoan parasites, such as *Plasmodium falciparum* or *Leishmania donovani*, have a significant health, social, and economic impact and threaten billions of people living tropical and sub-tropical regions of developing countries worldwide. The increasing range of parasite strains resistant to frontline therapeutics makes the identification of novel drug targets and the development of corresponding inhibitors vital. Post-translational modifications (PTMs) are important modulators of biology and inhibition of protein lipidation has emerged as a promising therapeutic strategy for treatment of parasitic diseases. In this review we summarise the latest insights into protein lipidation in protozoan parasites. We discuss how recent chemical proteomic approaches have delivered the first global overviews of protein lipidation in these organisms, contributing to our understanding of the role of this PTM in critical metabolic and cellular functions. Additionally, we highlight the development of new small molecule inhibitors to target parasite acyl transferases.

Key words: acyl transferase, palmitoylation, post-translational modification, protozoan parasites, protein lipidation, small molecule inhibitor, proteomics, NMT, *N*-Myristoyl transferase

INTRODUCTION

Infections with protozoan parasites of the genera *Plasmodium*, *Leishmania*, *Toxoplasma*, and *Trypanosoma* are among the most prevalent diseases in developing countries. Transmission of *Plasmodia* to human hosts through the bites of infected female *Anopheles* mosquitoes results in the acute febrile illness malaria. In 2015, 95 countries reported ongoing transmissions, resulting in half of the world's population (3.2 billion people) being at risk of malaria. *P. falciparum* and *P. vivax* pose the greatest threats with *P. falciparum* being responsible for most malaria-related deaths and *P. vivax* being the most dominant malaria parasite outside of sub-Saharan Africa (WHO, 2015). Protozoan parasites of the genus *Leishmania*, transmitted by the female sand fly, cause the spectrum of diseases known as the Leishmaniases. Symptoms range from skin ulcers with permanent scars to the swelling of the spleen and liver. Leishmaniases have been reported in Asia, Africa, South and Central America, and southern Europe, with 20-30,000 deaths annually (WHO, 2016a). Toxoplasmosis results from an infection with *Toxoplasma gondii*, transmitted through poorly cooked food, excrements from infected animals, or during pregnancy. Although up to half of the world's population becomes infected at some point in their lives, the immune system can usually cope with the parasite (Flegr *et al.*, 2014). However, toxoplasmosis can cause miscarriage during pregnancy or cause serious infections of the lungs or brain in people with a weak immune system (Jones *et al.*, 2014). Another well-known disease caused by a protozoan parasite is human African trypanosomiasis (HAT) which is caused by *Trypanosoma brucei*. Also known as sleeping sickness, HAT is transmitted by the tsetse fly and occurs in 36 sub-Saharan African countries (WHO, 2016b). These diseases have serious and sometimes lethal consequences if untreated. One major challenge is the increasing number of strains that have developed resistance against frontline therapeutics, including chloroquine, pyrimethamine/sulfadoxine, and artemisinin in the case of malaria (Sinha *et al.*, 2014; Mbengue *et al.*, 2015), pentavalent antimonials in the case of Leishmaniasis (Hajjaran *et al.*, 2016), and melarsoprol and pentamidine in the case of HAT (Baker *et al.*, 2013; Graf *et al.*, 2016). This highlights an urgent need for new validated drug targets and lead compounds.

Post-translational modifications (PTMs) are covalent and predominantly enzymatic modifications of proteins that occur during or after protein translation. One such PTM is the attachment of lipids (e.g. myristic or palmitic acid) to protein N-termini or side chains. Lipidation is typically catalysed by an acyl transferase that utilises the coenzyme A activated lipid as a cofactor. In this review we will focus on two protein lipidations: *S*-acylation, the attachment of a long chain saturated fatty acid (mainly C16:0, palmitate) to a cysteine side chain via a thioester linkage, and *N*-myristoylation. *N*-Myristoylation is catalysed by an acyl transferase, *N*-myristoyl transferase (NMT), which attaches myristic acid to the N-terminus of a specific set of protein substrates in lower and higher eukaryotes, thereby forming an amide bond between the 14-carbon saturated fatty acid and an N-terminal glycine (Boutin, 1997). The corresponding PTM occurs co-translationally (Wilcox *et al.*, 1987) and is generally known to be involved in protein-protein interactions, the association of proteins with membranes, and protein stability (Resh, 1999, 2006; Wright *et al.*, 2009). Until recently, relatively little was known about the protein substrates of NMT in protozoan parasites. In *P. falciparum*, a single NMT isoform was discovered that was shown to myristoylate GAP45 (host cell invasion; (Rees-Channer *et al.*, 2006)), CDPK1 (life cycle regulation; (Möskes *et al.*, 2004)), ARF1 (trafficking; (Leber *et al.*, 2009)) and AK2 (energy metabolism; (Rahlfs *et al.*, 2009)). In *Leishmania*, ARL1 (trafficking; (Sahin *et al.*, 2008)), HASPB (unknown function; (Sádlová *et al.*, 2010)) and PPEF (protein phosphatase; (Mills *et al.*, 2007)) have been reported to be myristoylated, amongst others. Our understanding of the significance of this PTM has been greatly enhanced over the last five years by global chemical proteomic strategies, as discussed in the next two sections ('APPROACHES FOR GLOBAL PROFILING OF PROTEIN LIPIDATION' and 'APPLICATION OF GLOBAL LIPIDATION MAPPING TOOLS IN PARASITES'). NMT had been identified as a likely essential protein and potential drug target as early as 2000 by

Holder *et al.* for *P. falciparum* (Gunaratne *et al.*, 2000) and 2003 by Price *et al.* for *L. major* and *T. brucei* (Price *et al.*, 2003). Since then, a variety of different small molecule inhibitors have been reported, and recent developments will be discussed in the last section ('INHIBITORS OF PROTEIN LIPIDATION IN PROTOZOAN PARASITE').

Chemical proteomic approaches have also recently revealed widespread protein *S*-acylation in protozoan parasites. Palmitoylacyltransferases (PATs) catalyse *S*-acylation but the consensus sequence for this modification is even more poorly defined than that for *N*-myristoylation, the substrate specificities of the multiple PATs in any one organism are not entirely defined. The dynamic, reversible nature of some *S*-acylation events makes unravelling the state and function of this modification particularly challenging. PATs are integral membrane proteins with a characteristic DHHC motif within a cysteine-rich domain (CRD) important for catalysis. They localise to membranes of different subcellular compartments via targeting motifs that are not yet understood, and that differ between species. There are 12 PATs in *P. falciparum*, 11 in the rodent model *Plasmodium berghei*, and 18 in *T. gondii*, some of which appear to be essential for parasite survival (Frénal *et al.*, 2013). Furthermore, several recent studies indicate that PATs play stage-specific roles in parasite biology (Beck *et al.*, 2013; Santos *et al.*, 2016; Hopp *et al.*, 2016; Tay *et al.*, 2016). In trypanosomatids, bioinformatic searches for the DHHC-CRD motif have identified 12 predicted PATs in *T. brucei* (Emmer *et al.*, 2009), 15 in *T. cruzi*, and 20 in *L. major* (Goldston *et al.*, 2014). Interestingly, RNAi knockdown of individual PATs does not affect *T. brucei* parasite growth in culture, and although this does not exclude a role in virulence or infection, this suggests that there is redundancy and cross-over in PAT substrate specificity (Emmer *et al.*, 2011). The study of PAT function is hindered by the fact that, in contrast to *N*-myristoylation, there are no specific chemical inhibitors of PATs. The druggability of these enzymes should be a high priority for further study.

APPROACHES FOR GLOBAL PROFILING OF PROTEIN LIPIDATION

A given PTM is typically of low abundance and often very difficult to detect and quantify directly in the context of a whole proteome. Modified proteins are therefore usually enriched before downstream analysis. However, there are no reliable affinity-based methods to globally enrich lipidated proteins, and historically lipidation has been studied on a protein-by-protein basis using metabolic labelling with poorly-sensitive radiolabelled lipid analogues in conjunction with immunoprecipitation. Either specific and highly sensitive antibodies are required, making the approach low-throughput, or the protein of interest must be overexpressed, raising questions over the validity of the result in native systems. Computational approaches to predict lipidation of proteins also exist (Maurer-Stroh *et al.*, 2002; Bologna *et al.*, 2004; Ren *et al.*, 2008). However, the sequence motifs are not clearly defined and bioinformatics tools rely on learning sets derived from species such as yeast that may not be transferable to protozoan parasites.

Here we discuss two modern techniques that have been effectively applied in protozoan parasites to globally enrich and identify lipid modified proteins. The first exploits the chemistry of the PTM linkage, and the second uses tagged lipid analogues that are metabolically incorporated into proteins in the cell. Both approaches have benefited hugely from parallel advances in quantitative proteomics methods and the increasing sensitivity of mass spectrometry (MS) instruments.

Acyl biotin exchange (ABE) chemistry is a well-established technique for detecting *S*-acylation of proteins (Roth *et al.*, 2006). ABE is a biotin-switch method that exploits our ability to selectively capture thiols and cleave thioesters to install a biotin affinity tag onto proteins at the site of *S*-acylation. A protein lysate is treated with a thiol-reactive reagent such as *N*-ethyl maleimide (NEM) to block free thiols. Subsequently, thioesters (including *S*-acyl chains) are selectively cleaved with

hydroxylamine (HA; **Fig. 1**). Treatment with the disulphide-forming reagent HPDP-biotin labels the liberated thiols with biotin. A control portion of the lysate is not treated with HA, and therefore lacks the biotin tag. The two samples are then incubated with an affinity resin (e.g. avidin agarose) and enriched proteins subjected to proteolytic digest. The corresponding peptide fragments are identified by mass spectrometry-based proteomics and the hits of the two samples are compared. The disulfide linkage between the biotin group and the modified peptide can also be cleaved to enable identification of the *S*-acylation site. Variations on this technique include acyl-RAC (resin-assisted capture) (Forrester *et al.*, 2011), where newly exposed thiols derived from thioesters are directly captured on a resin – combining the labelling and enrichment steps – and the recently reported acyl-PEG exchange (APE) (Percher *et al.*, 2016), which installs a polyethylene glycol (PEG) tag in place of biotin; the mass shifts from the PEG group are readily detectable through gel electrophoresis and Western blot, and can be used to determine levels of *S*-acylation.

ABE and related approaches are powerful methods for profiling *S*-acylation. However, ABE provides no information on the nature of the PTM that was incorporated at the thioester site (such as the acyl chain length), is limited to thioester-linked fatty acylations, and cannot distinguish acylation from any other thioester-linked modifications. Incomplete blocking of thiols of abundant proteins can also cause problems of background noise. Metabolic tagging with click chemistry (MTCC) is a complementary approach that is more generally applicable to a variety of lipid modifications (Tate *et al.*, 2015).

The principle behind MTCC is to use the endogenous machinery of the cell to install a latent chemical tag via the PTM: tagged analogues of the PTM of interest are fed to live cells and incorporated into modified proteins (**Fig. 2**). The tag must be very small in order to be tolerated by the enzymes that catalyse modification, biorthogonal such that it reacts minimally with the cellular environment, yet reactive enough to act as a chemical handle for downstream capture (with fluorophores or affinity handles such as biotin) and analysis of tagged proteins. The 'capture' chemistry most widely used is the copper-catalysed ligation of a terminal alkyne with an azide (a click reaction, also referred to as CuAAC). Although both azido- and alkynyl-fatty acids have been used in metabolic tagging approaches, alkyne-modified lipids are often preferred – mainly due to the empirical observation that this orientation (alkyne on lipid, azide on capture reagent) leads to lower background labelling. MTCC has been applied to detect *N*-myristoylation and *S*-palmitoylation of proteins in protozoan parasites, using the tools shown in **Figure 2**.

A significant advantage of MTCC is that in principle a tool can be designed to address any PTM in an unbiased way. For example, a myristic acid mimic such as YnMyr (**1**) or AzMyr (**3**) (**Fig. 2B**) could be incorporated onto protein N-termini (as for NMT-catalysed *N*-myristoylation), or onto other sites, such as *S*-acylation sites. Tagged analogues should therefore enable detection of less common lipid modifications, such as lysine myristoylation. However, identification of the site of modification can be complex because the biotin-lipid-peptide fragment resulting from protein digest is difficult to detect by mass spectrometry, or remains anchored to the resin if the proteins are digested on-bead. To tackle this problem, several groups have developed cleavable biotin-azide reagents that allow selective release of the lipidated peptide (e.g. (Broncel *et al.*, 2015)). The extent to which lipid analogues are metabolised by the biological system is difficult to assess and remains largely unexplored; this complicates analysis but also provides opportunities to use these tools to map lipid metabolism in diverse systems in the future. As we shall illustrate in the next section, combining ABE and/or MTCC with specific chemical inhibitors or genetic knockdowns of lipid transferase enzymes has proven to be a particularly powerful approach for globally identifying lipidated proteins and assessing the druggability of their cognate transferases.

APPLICATION OF GLOBAL LIPIDATION MAPPING TOOLS IN PARASITES

Over the past 5 years, both ABE and MTCC have been applied in parasites to discover and validate protein lipidation and to probe its inhibition. Prior to the development of these techniques only a handful of proteins had been shown to be lipidated in these organisms, and in many cases only using genetically engineered over-expression systems (reviewed in (Tate *et al.*, 2014). Here we discuss recent applications of these techniques in apicomplexan parasites (*Plasmodia*, *Toxoplasma*) and in trypanosomatids (*Trypanosoma*, *Leishmania*).

Malaria parasites

In 2012, Jones *et al.* reported the first global study of *S*-palmitoylation in the asexual stage of the malaria parasite *P. falciparum*, by applying both MTCC with the well-established palmitate analogue 17-ODYA (**4**) (**Fig. 2**) and ABE (Jones *et al.*, 2012). Quantitative comparison between sample and control in both approaches was carried out using SILAC (stable isotope labelling of amino acids in culture) and the study identified >400 potential palmitoylated proteins. The authors combined ABE with the compound 2-bromopalmitate (2-BP) to analyse the degree to which specific palmitoylations are dynamic. A significant caveat to these results is that 2-BP is **not** a specific thioesterase inhibitor and has broad non-specific reactivity, including particularly on lipid metabolic pathways (Coleman *et al.*, 1992; Zheng *et al.*, 2013; Davda *et al.*, 2013); the continued use of this molecule despite its potent promiscuity is symptomatic of the lack of well-characterised specific inhibitors for palmitoyltransferases. Despite this issue, the study of Jones *et al.* was nevertheless a landmark application of ABE and MTCC in a protozoan parasite, and elegantly demonstrates the complementarity of the two techniques (**Fig. 3A**).

Our lab and others have worked extensively on *N*-myristoylation in malaria and other biological systems, both in terms of inhibitor development (see section 'INHIBITORS OF PROTEIN LIPIDATION IN PROTOZOAN PARASITES') and to globally identify myristoylated proteins. MTCC relies on the cellular machinery to take up fatty acid analogues, convert them into substrates for the acyl transferase (the acyl-CoA thioesters) and incorporate them enzymatically. Early work demonstrated that NMTs will accept azide- and alkyne-tagged myristate mimics *in vitro* and incorporate them into peptide substrates (Heal *et al.*, 2008). Furthermore, the binding mode of YnMyr-CoA crystallised in the active site of *P. vivax* NMT (**Fig. 4A**) is nearly identical to the conformation adopted by Myr-CoA (Wright *et al.*, 2014). MTCC with YnMyr (**1**) was applied to identify myristoylated proteins in asexual stage *P. falciparum* schizonts, revealing not only putative *N*-myristoylated proteins but also proteins known to be modified with a glycosylphosphatidylinositol(GPI) anchor (**Fig. 4B**). Jones *et al.* found that 17-ODYA (**4**) is also incorporated into *Plasmodium* GPI anchors (Jones *et al.*, 2012). These results are not surprising, since *Plasmodium* GPI anchors are known to incorporate both fatty acids, and illustrate the versatility of the lipid analogues which are readily incorporated by the GPI biosynthetic machinery. *N*-Myristoylation is thought to take place mostly on the N-terminal glycine of substrate proteins. To confirm that YnMyr (**1**) was attached to these sites, a cleavable azido-biotin reagent (Broncel *et al.*, 2015) was used: after pull-down of tagged and biotin labelled proteins, tryptic digest released both the unmodified and modified peptides (**Fig. 2A**) (Wright *et al.*, 2014). Indeed, around 30 modified protein N-termini were detected in this case, providing conclusive evidence for the site-specific attachment of YnMyr (**1**) to these proteins.

Identifying the mode of action of drugs and small molecules of interest in a live cell context is very challenging, particularly in protozoan parasites. We next exploited our robust and rapid MTCC approach to assess whether NMT inhibitors were acting on-target in the parasite, using both previously reported *T. brucei* inhibitors (**Fig. 10A**, compounds **19** and **20**) (Frearson *et al.*, 2010; Brand

et al., 2012) and a novel chemically distinct series developed in-house (**Fig. 9A**, compounds **15** and analogues) (Rackham *et al.*, 2014). All five compounds specifically inhibited incorporation of YnMyr (**1**) into *N*-myristoylated proteins, and furthermore the in-cell dose-responses calculated from levels of YnMyr (**1**) incorporation correlated well with EC_{50} for parasite growth inhibition (**Fig. 4C**). These experiments therefore demonstrated direct engagement of compounds with NMT in cells and linked parasite death to loss of substrate protein myristoylation. With validated tools in-hand, the phenotype of NMT inhibition in the malaria parasite could be characterised (Wright *et al.*, 2014).

YnMyr (**1**) has proven a versatile tool in *Plasmodium* species, and this analogue has also been applied in the mouse malaria parasite *P. berghei* to detect myristoylation of specific proteins involved in sexual development: two inner-membrane complex proteins (Poulin *et al.*, 2013), and two protein phosphatases (Guttery *et al.*, 2014).

Toxoplasma gondii

Palmitoylation has been implicated in the intracellular life cycle of the related apicomplexan parasite *T. gondii*. For example, a palmitoyl protein thioesterase was identified as a target for a small molecule enhancer of host cell invasion, suggesting that dynamic protein *S*-acylation may play an important regulatory role in this process (Child *et al.*, 2013). The latter study also used 17-ODYA (**4**) (**Fig. 2B**) to verify *S*-palmitoylation of specific proteins associated with the enhanced invasive phenotype. Building on this work, Foe *et al.* carried out a global analysis of 17-ODYA (**4**) tagged proteins in *T. gondii* extracellular invasive stages (Foe *et al.*, 2015). Recognising that the lipid probe may be incorporated into multiple sites in addition to *S*-palmitoylated cysteines (such as GPI anchored proteins), the authors also compared samples treated with or without hydroxylamine (HA). This treatment should selectively cleave thioesters, releasing only *S*-acylation sites. Quantitative label-free proteomics was used to generate hits within these two experimental set-ups. Comparing the results revealed a final list of ~280 high confidence *S*-palmitoylated proteins in *T. gondii*. Follow-up analysis of one newly identified *S*-palmitoylated protein, AMA1, which is known to be associated with invasion, showed that one cysteine in particular is likely *S*-acylated. *S*-Acylation did not appear to be related to AMA1 localisation, but a subtle effect on the rate of secretion of microneme proteins was observed. Interestingly, the *S*-palmitoylated proteome of *T. gondii* showed limited overlap with palmitoylated orthologues in *P. falciparum*, perhaps reflecting differences in the life stages analysed, or indicating that most palmitoylation is organism-specific (Foe *et al.*, 2015).

The complementary approach of ABE was also recently applied to *T. gondii*. Semi-quantitative comparisons of samples treated with and without HA resulted in >400 protein hits (Caballero *et al.*, 2016). Around half of these were also identified by Foe *et al.* using their complementary approach (**Fig. 3B**). Although only around 50 of the proteins identified by Caballero *et al.* were found in two biological replicates, suggesting that there is quite some variability in the ABE technique, again around half matched to high confidence hits from Foe *et al.* (**Supplementary Table S1**). Together, these two studies have provided a wealth of data on potential palmitoylated proteins in *T. gondii*.

Comparisons across the Apicomplexa

Foe *et al.* compared their *T. gondii* palmitome dataset (17-ODYA (**4**)) with the *P. falciparum* datasets (17-ODYA (**4**) plus ABE) of Jones *et al.* by identifying orthologues in these two related species. They noted a poor overlap. We added the data of Caballero *et al.* to this analysis, comparing the aggregate of all three studies: Of ~320 putative palmitoylated proteins identified in *P. falciparum* that have *T.*

gondii orthologues, 141 now have some evidence for *S*-acylation from either ABE or 17-ODYA (**4**) analyses in *T. gondii* (**Fig. 3C**). As has been noted by the studies described above, it is clear that MTCC and ABE identify not only overlapping but also distinct subsets of the palmitome (and therefore also distinct sets of false positives), and there is value to using both methodologies in combination. In addition, by comparing the *P. falciparum* data from our myristoylation study with the palmitoylation analyses, we identify 10 likely dually acylated proteins in the parasite (**Fig. 3D**). The Apicomplexa comparisons are given in **Supplementary Table S1**, although it should be noted that exact numbers in these comparisons are dependent on how the analysis is carried out: orthologues frequently do not map one-to-one and mass spectrometry data often cannot distinguish between closely related proteins, which is a widely studied problem in protein inference (Li and Radivojac, 2012).

Trypanosoma brucei

MTCC was first applied in the sleeping sickness parasite *T. brucei* to validate the *N*-myristoylation of a particular protein of interest, ARL6 (Price *et al.*, 2012), which had a putative role in intracellular protein trafficking. Following metabolic tagging with YnMyr (**1**) (**Fig. 2B**), ARL6 was immunoprecipitated from lysate with a specific antibody. Subsequent labelling with a fluorescent azide reagent allowed detection of the modified ARL6 in-gel. Expanding this approach, a global profile of *N*-myristoylated proteins was performed comparing both bloodstream and insect stages of *T. brucei* (**Fig. 5A**) (Wright *et al.*, 2016). Out of ~100 robustly enriched proteins in each life stage, roughly half possessed the canonical N-terminal glycine myristoylation motif. Others are known to be GPI anchored or *S*-acylated, consistent with the frequent observation that *S*-acylation is more permissive of fatty acid chain length in many eukaryotic systems – i.e. both myristate and palmitate (and their corresponding alkynyl-analogues) can be incorporated onto cysteine side chains (**Fig. 5B**). Indeed, longer chain palmitate analogue YnPal (**2**) tagged a distinct but overlapping set of proteins in *T. brucei* (Wright *et al.*, 2016). Comparison of the MTCC-derived dataset with the results of an earlier ABE experiment conducted in *T. brucei* by Emmer *et al.* (Emmer *et al.*, 2011) revealed some overlap but also differences (**Fig. 6A**); these are likely the result of both biological (host versus insect form parasites) and technical (MTCC versus ABE) differences in the two studies. Interestingly, YnMyr (**1**) turned out to be toxic at extended incubation times to bloodstream but not insect forms of *T. brucei* (Wright *et al.*, 2016). This observation is not without precedent (Doering *et al.*, 1994) and is likely related to effects on the GPI anchor pathway, which is highly dependent on myristate incorporation and crucial for *T. brucei* host stages (Ferguson *et al.*, 1985).

Unlike for *S*-acylation where multiple, possibly redundant, palmitoylacyltransferase (PAT) enzymes exist, NMT appears to be the sole enzyme responsible for protein *N*-myristoylation. The enzyme has a quite narrow substrate specificity for myristoyl-CoA and closely related analogues (Wright *et al.*, 2009). Furthermore, whilst there are no specific chemical tools for the inhibition of PATs, for NMT there are several well-characterised molecules available (see section 'INHIBITORS OF PROTEIN LIPIDATION IN PROTOZOAN PARASITE'). The *T. brucei* NMT inhibitors reported by Frearson *et al.* (Frearson *et al.*, 2010; Brand *et al.*, 2012) specifically reduced YnMyr incorporation into *N*-myristoylated, but not GPI anchored proteins in BSF parasites (**Fig. 5B**), demonstrating target engagement in cells. We therefore applied these compounds to simplify the interpretation of the complex YnMyr (**1**) tagged proteome data, and determine which proteins were true NMT substrates. Parasites were treated with different concentrations of two inhibitors with very different potency, and then proteins tagged with YnMyr (**1**). After enrichment, quantitative label-free proteomics was used to assess which proteins had reduced YnMyr (**1**) incorporation in response to inhibition. This analysis revealed ~50 high confidence NMT substrates; for many of these the YnMyr (**1**)-modified N-terminal glycine-containing peptide was also identified via cleavable reagents.

Trypanosoma cruzi

NMT is also under investigation as a potential drug target in *T. cruzi*. Although NMT inhibitors developed against *T. brucei* were significantly less efficacious in this organism, Roberts *et al.* showed that the compounds inhibited parasite growth and reduced incorporation of azido-myristate mimic AzMyr (**3**) (**Fig. 2B**) in a dose-dependent manner (as read-out by in-gel fluorescence), suggesting that NMT is druggable in this system (Roberts *et al.*, 2014). The authors recently followed this with a study applying AzMyr (**3**) to identify *N*-myristoylated proteins in *T. cruzi* (Roberts and Fairlamb, 2016). They used both label-free and SILAC quantification and focused on *N*-myristoylation by treating samples with HA to cleave *S*-acylation sites. Additionally, they applied two concentrations of their well-characterised NMT inhibitor. This analysis identified ~50 high confidence *N*-myristoylated proteins in the parasite; more than half of these had homologues identified as NMT substrates in the *T. brucei* YnMyr study (Wright *et al.*, 2016) (**Fig. 6B**). Related compounds were also recently shown to act on-target in *T. cruzi* using a gel-based fluorescent read-out after AzMyr (**3**) tagging (Herrera *et al.*, 2016).

Leishmania donovani

The extent of protein lipidation in *Leishmania* species was similarly poorly characterised until recently. We applied YnMyr (**1**)-based MTCC with label-free quantitative proteomics to assess the potential of NMT as a drug target in *L. donovani* (Wright *et al.*, 2015). As in *T. brucei*, YnMyr (**1**) was incorporated into likely *N*-myristoylated, *S*-acylated and GPI anchored proteins, as well as into surface glycolipids that are prevalent in trypanosomatids. A quantitative chemical proteomics based comparison of YnMyr (**1**) tagged proteins revealed an overlap of 67% between insect (promastigote) and mammalian host (amastigote) stages of *Leishmania* parasites, a reflection of their distinct metabolism, and proteome profiles. In addition to enabling study of the different life stages *ex vivo*, the high sensitivity of MTCC even allowed detection of YnMyr (**1**) incorporation into native levels of the well-studied *N*-myristoylated protein HASPB in macrophages infected with amastigotes.

Taking a similar approach to *T. brucei*, the effects of NMT inhibition on YnMyr (**1**) modification of each protein were assessed using inhibitor **19** and its *N*-methylated analogue (**19a**). These two compounds have nM potency against *Ld*NMT but dramatically different potencies in cells, with the latter (**19a**) nearly 50-fold more active against amastigotes than the former (**19**). Whilst this discrepancy could be due to compound uptake, metabolism, or efflux, it also raised the question of whether both compounds were truly acting on-target. YnMyr (**1**) tagging was performed in the presence of the two compounds at approximately their EC_{50} values, and revealed the same loss of labelling of specific bands (**Fig. 7A**). Further quantitative chemical proteomics confirmed this result: YnMyr (**1**) tagging of the same group of proteins was sensitive to NMT inhibition, demonstrating that both inhibitors engage NMT in live cells. As in other systems, combining chemical inhibition and MTCC proved a powerful approach for dissecting the complex lipidation patterns and ~30 proteins were identified as high confidence NMT substrates (**Fig. 7B**). In addition to proteins involved in trafficking, protein phosphorylation, Golgi function and proteasomal degradation, just over half of the hits are completely uncharacterised. Again, there was good overlap with high confidence *T. brucei* myristoylated orthologues (**Fig. 6C**).

Based on this study, it is clear that on-target NMT inhibitors selectively reduce YnMyr (**1**) incorporation into specific proteins, but do not affect tagging of others (GPI anchored, *S*-acylated). Indeed, we observed this across *Plasmodia*, *Trypanosoma*, and *Leishmania* parasites, as described

above. Since YnMyr (**1**) incorporation can be assessed on-gel, MTCC provides a rapid method to screen for on-target activity of promising NMT inhibitors in these organisms.

Comparisons across the trypanosomatids

The three studies analysing *N*-myristoylation using MTCC in *T. brucei*, *T. cruzi*, and *L. donovani*, all applied well-characterised inhibitors from the series reported by Frearson *et al.* in quantitative proteomics experiments to define NMT substrates. This is important because it enables one to distinguish between proteins that incorporate Yn/AzMyr (**1**/**3**) at *S*-palmitoyl or other sites, from those truly N-terminally myristoylated by NMT. With this piece of information and the *T. brucei S*-palmitoyl proteomics studies of Wright *et al.* (YnPal MTCC) and Emmer *et al.* (ABE), candidate proteins for dual acylation in this organism can be identified (**Fig. 6D** and **Supplementary Table S2**). This analysis confirms well-validated examples (e.g. dual acylation of metacaspase 4 and the family of flagellar calcium-binding proteins (Godsel, 1999; Proto *et al.*, 2011)) and reveals further avenues of study. For example, the data suggest dual acylation of an ADP-ribosylation factor, two protein phosphatases, and numerous proteins involved in fatty acid metabolism, although whether the latter are acylated or bind lipids as part of their catalytic activity remains to be investigated.

To identify conserved *N*-myristoylated proteins, the set of high confidence *T. brucei* NMT hits were analysed for orthologues in *T. cruzi* and *L. donovani* and cross-compared with *N*-myristoyl datasets from those organisms. There was indeed good overlap between datasets (**Fig. 6B & C**, **Supplementary Table S2**), perhaps due to similarity in experimental protocols, as well as the close relatedness of the organisms. The 10 proteins identified across all three organisms (**Fig. 6E**) are likely only a snapshot of the conserved *N*-myristoylated proteome, but proteins with functions as diverse as protein degradation (the proteasome subunit), phosphorylation (two protein phosphatases), trafficking (two ARFs), and metabolic regulation (AMPK subunit) can be identified.

INHIBITORS OF PROTEIN LIPIDATION IN PROTOZOAN PARASITES

Considering that acyl transferases catalyse the attachment of modifications that are essential for several vital biological processes in protozoan parasites, the development of corresponding selective and potent small molecule inhibitors could significantly contribute to the limited arsenal of therapies currently available. During the last decade, a variety of different small molecule inhibitors has been identified. The last few years have seen further development of the corresponding scaffolds, as summarised below.

Plasmodium and Leishmania

In order to identify *P. falciparum* and *P. vivax* NMT (*Pf*NMT and *Pv*NMT) inhibitor scaffolds, two high throughput screening (HTS) approaches were performed. For the first HTS a 150000 compound library was screened with our collaborators at Pfizer in a radioactive scintillation proximity assay (SPA) against *Pf*NMT and *Leishmania donovani* NMT (*Ld*NMT) (Bell *et al.*, 2012), while a second HTS was performed in collaboration with MRC Technology (MRCT) and used a 60,000 compound library in a fluorescence based assay against *Pv*NMT (Goncalves *et al.*, 2012b). The fluorescence-based assay format exploits the reaction between the thiol reactive 7-diethylamino-3-(4-maleimido-phenyl)-4-methylcoumarin (CPM) and the free CoA liberated during the enzymatic acyl-transfer (Goncalves *et al.*, 2012a). Both high throughput screens identified hits in a variety of structural series. Thereby, the

SPA based HTS resulted in the identification of excellent *Pf*NMT inhibitor scaffolds that were further progressed during the last four years. The most promising hit compound of the MRCT HTS was further progressed in a compound series based on a quinoline scaffold (**Fig. 8A**, compound **5**) characterised by micromolar IC_{50} against *Pv*NMT and a moderate selectivity over human NMT (*Hs*NMT) (Goncalves *et al.*, 2012b). The HTS of the Pfizer library against *Ld*NMT successfully identified four series (**Fig. 8B** aminoacylpyrrolidines – compound **7**, piperidinylindoles – compound **8**, thienopyrimidines, and biphenyl derivatives) with good to excellent selectivity over all other NMTs tested (Bell *et al.*, 2012). The binding mode of all four inhibitor classes was subsequently determined by co-crystallisation with *Ld*NMT and/or *L. major* NMT (*Lm*NMT) (**Fig. 8B**; (Brannigan *et al.*, 2014). All inhibitors, apart from the aminoacylpyrrolidines, interact via a basic centre with the C-terminal carboxylate of the enzyme. In the case of **7** and **9**, the corresponding interaction is mediated by the hydroxyl substituent. Moreover, all compounds show significant interactions with aromatic side chains of Phe90, Tyr217, and Tyr345, and exhibit an additional set of individual interactions. These structural insights were used in a subsequent structure-guided fusion of scaffolds **7** and **8** (Hutton *et al.*, 2014). The product (**Fig. 8B**, compound **9**) of the inhibitor hybridization exhibits a 40-fold increased potency with good selectivity over *Hs*NMT. However, one major issue with all three inhibitors (**7**, **8**, and **9**) is the lack of cell based activity, which MTCC analysis suggests is due to poor cellular uptake limiting access to the target in cells (Hutton *et al.*, 2014; Paape *et al.*, 2014).

In parallel an alternative strategy was exploited to identify new *Pf*NMT inhibitors by testing the antimalarial potency of drug molecules that have already been evaluated by pharma companies as lead compounds for the treatment of other diseases. This so called 'piggyback' approach was based on a library of 43 inhibitors against NMT from *Candida albicans* (*Ca*NMT). Although four hits successfully reduced parasitaemia *in vitro*, the compounds exhibit a low ligand efficiency (LE) due to their high molecular weight and high lipophilicity relative to their low enzyme affinity (Bowyer *et al.*, 2007, 2008). Screening a second small library of 25 inhibitors of *Ca*NMT and *Trypanosoma brucei* NMT (*Tb*NMT) finally revealed RO-09-4609 (**10**) as a moderately selective hit compound. Further optimisation resulted in the development of an inhibitor series with a benzo[*b*]furan scaffold (**Fig. 9A**, compound **11**+**12**) that exhibits a 100-fold affinity improvement over the initial compound. Co-crystallisation of inhibitor **12** with *P. vivax* NMT (*Pv*NMT) revealed a competitive binding mode of the benzo[*b*]furan inhibitors with the peptide substrate (Yu *et al.*, 2012). The corresponding inhibitors are characterised by moderate enzyme affinity, and the LE was still too low to consider the series to be favourable for further optimisation. To overcome this issue, an inhibitor series based on a benzo[*b*]thiophene scaffold (**Fig. 9A**, compounds **13**-**15**) was developed to mediate improved π-interactions with two tyrosine residues due to the increased aromatic character of the thiophene moiety. Crystallography of these novel inhibitors with *Pv*NMT revealed an overlapping but distinct binding mode to the benzo[*b*]furanes, with the benzo[*b*]thiophene moiety being buried deeper within a hydrophobic pocket (Rackham *et al.*, 2013). The structure additionally showed that an appropriately positioned methoxyphenyl substituent should be able to interact with Phe105 and Ser319 of *Pv*NMT, thereby increasing the affinity due to further π-π interactions. This hypothesis was validated by increasing the linker length between the benzo[*b*]thiophene core and the methoxyphenyl substituent. The resulting inhibitor **14** exhibits a 6-fold increased affinity against *Pf*NMT (**Fig. 9A**; (Rackham *et al.*, 2014). However, one issue with the ester containing benzo[*b*]thiophenes is the high lipophilic ligand efficiency (LLE) value of e.g. 13.2 for **13**. Highly lipophilic compounds are more likely to partition from plasma to membranes and proteins and thereby exhibit an increased promiscuity and toxicity. The LLE value considers lipohilicity, affinity, and molecular size. Thereby, desirable leads exhibit an LLE of <10 (corresponding to LE > 0.3 and cLogP < 3) (Keserü and Makara, 2009). To significantly decrease the LLE and to further increase enzyme affinity, 1,3,4-oxadiazole was implemented as a bioisosteric replacement of the ester linker

moiety (Rackham *et al.*, 2014). The corresponding derivatives (**Fig. 9A**, compound **15**) showed a 100-fold improved enzyme affinity and a 100-fold decreased lipophilicity while retaining the selectivity over *Hs*NMT with respect to the first benzo[*b*]thiophene lead compound **13**. Apart from its antiparasitic *in vitro* activity, compound **15** is potent against four parasite strains, including two drug-resistant ones, and shows promising activity against liver stage (EC_{50} = 372 nM) parasites.

Scaffold simplification by substituting the bicyclic core with pyridyl (**Fig. 5A**, compound **16**) resulted in the most recently reported oxadiazole containing inhibitor series (Yu *et al.*, 2015). Remarkably, the scaffold-simplified inhibitors exhibit a similar binding mode in the *Pv*NMT crystal structure as the benzo[*b*]furane derivatives (**Fig. 9A**). The 1,2,4-oxadiazole is sandwiched between Y334 and Y211, while the pyridyl nitrogen of **16** additionally stabilises the enzyme-inhibitor complex via water-mediated hydrogen bonds with Y315. Strikingly, the 3-OMe phenyl moiety of compound **16** also overlays well with the quinoline scaffold of compound **5** (**Fig. 8A**). Exchanging the trimethylpyrazole with a quinolone moiety finally provided compound **17** (**Fig. 9A**) with an IC_{50} of 1.7 nM against *Pf*NMT and good cellular efficacy. The benzo[*b*]thiophene series was also routinely tested against *Ld*NMT. Remarkably, the affinity spectrum changes significantly if the bicyclic system is truncated to a monocyclic thiophene scaffold (Rackham *et al.*, 2015). Activity against human and *Plasmodium* NMTs decreases by almost two orders of magnitude while affinity against *Ld*NMT increases 8-fold. However, since thiophene moieties have been associated with P450 inhibition, a 1,3,4-oxadiazole containing 5-chlorophenyl derivative was obtained as optimum scaffold that shows no macrophage toxicity. However, the compound failed to inhibit axenic *L. donovani* amastigotes (leishmanial stage), likely due to difficulty accessing the target in this parasite. Therefore, further investigation of the physicochemical properties of this series is essential.

Finally, we also reported development of a *Pv*NMT and *Lm*NMT peptidomimetic inhibitor based on an fungal NMT inhibitor (Olaleye *et al.*, 2014). The structure of the peptide (**Fig. 9B**, compound **18**) comprises a Ser-Lys dipeptide, a C-terminal cyclohexyl moiety, and an aliphatic chain at the N-terminus. The resulting peptidomimetic is characterised by sub-micromolar potency against both enzymes and a marginal selectivity over *Hs*NMT. Interestingly, 20% of the electron density of the inhibitor-NMT complex structure corresponds to an *N*-myristoylated inhibitor product and the CoA by-product, providing the first direct structural evidence for a product complex in NMT (**Fig. 9B**). This complex is presumably formed *in situ* in the crystal, favoured by the high inhibitor occupancy in the solid state.

Toxoplasma

S-palmitoylation is a dynamic PTM that requires a corresponding acyl-protein thioesterase (APT) for the cleavage of the lipid thioesters. In *T. gondii*, TgPPT1/TgASH1 was recently identified as an orthologue of human APT1. This serine hydrolase can be inhibited by substituted chloroisocoumarin-, β-lactone-, and triazole urea-based inhibitors (Kemp *et al.*, 2013; Child *et al.*, 2013). Interestingly, these inhibitors *enhance* tachyzoite invasion. Although enhancers of invasion are not obvious therapeutic agents, Bogyo *et al.* speculated that the increase in number of host-cells infected by multiple parasites and the corresponding increase in the competition for resources within the infected cell might be an unconventional point of action for therapeutics, although further studies are required to test this hypothesis (Child *et al.*, 2013).

2-BP is another small molecule compound that is often incorrectly considered a global inhibitor of palmitoylation. Treatment of *T. gondii* with 2-BP resulted in altered gliding motility patterns of the parasite and a significant reduction of the invasion process (Alonso *et al.*, 2012), but as mentioned

above these findings should be interpreted carefully, and in full appreciation of the very promiscuous activity and high non-specific toxicity of 2-BP (Davda *et al.*, 2013).

Trypanosoma

Pyrazole sulphonamides are NMT inhibitors identified in an HTS against *Trypanosoma brucei* NMT (*Tb*NMT) by Wyatt *et al.* (Frearson *et al.*, 2010). Eight sulphonamide hits of this initial HTS were further investigated by Maldonado *et al.* using high content imaging and a metabolic labelling approach. The authors proved the on-target activity of three compounds in sub-micromolar concentrations also against *T. cruzi* NMT with very low cytotoxic side effects (Herrera *et al.*, 2016). The lead compound of the HTS, DDD85646 (**Fig. 10A**, compound **19**), shows excellent activity in mouse models during the hemolymphatic peripheral infection stage of *T. brucei* (stage 1) (Brand *et al.*, 2012). However, due to a low blood-brain barrier (BBB) permeability, the inhibitor is not active in the second stage during which the parasite enters the central nervous system (CNS) thereby giving rise to the classic symptoms of sleeping sickness. Therefore, Read *et al.* prepared modified pyrazole sulphonamides with a reduced polar surface and a capped sulphonamide group, significantly increasing the BBB permeability (Brand *et al.*, 2014). Their new lead compound (**Fig. 10A**, compound **20**) demonstrated partial efficacy in stage 2 mouse models. However, one issue is that the increased lipophilicity results in off-target effects and poor tolerability of the new lead compound.
Apart from the pyrazole sulphonamides, Gilbert *et al.* have progressed two further hits from the original HTS and developed a thiazolidinone (e.g. compound **21**) and a benzomorpholinone (e.g. compound **22**) series (**Fig. 10A**; (Spinks *et al.*, 2015). Like Read *et al.*, the authors aimed at the development of BBB permeable NMT inhibitors. Due to a lack of high-resolution structures of *Tb*NMT and a very high sequence homology of the binding pockets of *Tb*NMT and *Lm*NMT, the authors used *Lm*NMT as surrogate. Co-crystallography of the two new *Tb*NMT inhibitor classes with *Lm*NMT revealed that they are characterised by a different binding mode than the sulphonamides (**Fig. 10B**). The lead compound of the thiazolidine series (**Fig. 10A**, compound **21**) is characterised by good selectivity over *Hs*NMT, micromolar cellular efficacy, and a good LE value that indicates the potential of the series. The benzomorpholinone series (**Fig. 10A**, compound **22**) contains potent antiparasitic compounds with cellular potencies in the nanomolar range that exhibit BBB permeable compounds. However, the selectivity of the series has to be further improved to enable higher dose levels, and thereby maximising the chances of curing stage 2 infections.

CONCLUSIONS

Protein lipidation is an essential PTM for metabolic and cellular processes in protozoan parasites, and its modulation offers interesting opportunities for therapy. Therefore, an extensive investigation of the substrates of protozoan acyl transferases and the corresponding downstream effects of their inhibition is essential. In this context ABE and MTCC are powerful techniques that can be used to profile, image, and identify previously unknown lipidated proteins in a data-driven manner and without the need for specific antibodies or protein overexpression. ABE-type approaches can be used on any lysate without the need to optimise incorporation of an analogue and without the risk that the analogue will perturb the system. However, ABE is limited to *S*-acylation and provides no information on the lipid. MTCC approaches, in contrast, are unbiased and wide in scope. Only proteins dynamically modified during the incubation time with the analogue will be tagged and therefore identified – whilst this can be a potential limitation, more importantly it offers the opportunity for profiling *dynamic* lipidation through pulse-chase approaches. These technologies have dramatically increased our appreciation of the extent of protein lipidation in parasites and

demonstrate that targeting these modifications could have therapeutic value. The identification of small molecule inhibitor scaffolds that inhibit protozoan acyl transferases with high selectivity over the corresponding human enzymes is an important consideration for the development of therapies. In the case of *Plasmodium* and *Leishmania*, pyridyl, 1,3,4-oxadiazole containing 5-chlorophenyl, and peptidomimetic based scaffolds show promising characteristics and good cellular efficacy, including against liver stage malaria parasites. In the case of *Trypanosoma*, pyrazole sulphonamides, thiazolidinone and benzomorpholinone inhibitors are potent antiparasitic compounds; however, BBB permeability and selectivity needs to be further improved to increase their efficacy against stage 2 of *T. brucei* infection. Bringing together lipid profiling technologies and medicinal chemistry efforts, MTCC platforms in particular have been successfully used to demonstrate the on-target mode of action of NMT inhibitors in live parasites.

Evidence from analytical tools has accumulated to the point where *S*-acylation must be considered a major regulatory pathway in all eukaryotes (Resh, 2016). The enzymes involved in removal of this modification come from the superfamily of serine hydrolases, and selective small molecule inhibitors are available for some of these enzymes. Their inhibition can lead to interesting and unexpected phenotypes, as mentioned above, and further characterisation of their apparently broad substrate scope and complex localisation will be important in validating them as potential drug targets. In contrast, the diverse class of protein *S*-palmitoyl transferases (PATs), including >20 genes in humans, has yet to yield to small molecule inhibitor discovery, and the chemical tools available for PATs are effectively non-existent. Indeed, the continued use of 2-BP due to its commercial availability is to greatly compound the challenges of the field due to the exceptional promiscuity of this molecule, as noted above. Robust and widely-applicable CRIPSR-Cas gene-knockout approaches will be an important enabling tool to unpick the roles of PATs in parasites and in the host, but the discovery of cell-active inhibitors selective for the class, or for members of the class, would be transformative for the field, and should be pursued as a high priority.

In contrast, the scope for NMT as a target in eukaryotic pathogens is very clear, and may be very broad, as recently demonstrated for helminths (Galvin *et al.*, 2014). The availability of multiple potent inhibitor series and powerful tools to analyse PTMs in living systems greatly enhances the opportunities for drug development against this target. With the exception of *T. brucei*, which is rapidly killed by NMT inhibition due to its exceptional reliance on myristoylation-dependent trafficking, NMT inhibition has a quite extended mode of action. This is hypothesised to be due to an indirect dependence on protein degradation: myristoylated proteins that were present prior to inhibition will typically need to undergo some degree of degradation in order for inhibition of co-translational myristoylation to impact viability. Careful consideration of compound uptake in cells, distribution/pharmacokinetics and pharmacodynamics (the dynamics of target engagement) will be required to realise the potential of NMT inhibitors as antiparasitic agents, and research towards this objective continues in our labs, in collaboration with other research groups.

FINANCIAL SUPPORT

Financial support by Medicines for Malaria Venture (MMV) is gratefully acknowledged, and from the Engineering and Physical Sciences Research Council (EPSRC, grant EP/F500416/1).

ACKNOWLEDGEMENTS

The authors are grateful to the anonymous reviewers of this manuscript for suggesting the detailed and informative analyses presented in Figures 3 and 6.

REFERENCES

Alonso, A. M., Coceres, V. M., De Napoli, M. G., Nieto Guil, A. F., Angel, S. O. and Corvi, M. M. (2012). Protein palmitoylation inhibition by 2-bromopalmitate alters gliding, host cell invasion and parasite morphology in *Toxoplasma gondii*. *Molecular and Biochemical Parasitology* **184**, 39–43. doi:10.1016/j.molbiopara.2012.03.006.

Baker, N., de Koning, H. P., Mäser, P. and Horn, D. (2013). Drug resistance in African trypanosomiasis: the melarsoprol and pentamidine story. *Trends in parasitology* **29**, 110-118. doi:10.1016/j.pt.2012.12.005.

Beck, J. R., Fung, C., Straub, K. W., Coppens, I., Vashisht, A. A., Wohlschlegel, J. A. and Bradley, P. J. (2013). A Toxoplasma Palmitoyl Acyl Transferase and the Palmitoylated Armadillo Repeat Protein TgARO Govern Apical Rhoptry Tethering and Reveal a Critical Role for the Rhoptries in Host Cell Invasion but Not Egress. *PLoS Pathogens* **9**, e1003162. doi:10.1371/journal.ppat.1003162.

Bell, A. S., Mills, J. E., Williams, G. P., Brannigan, J. A., Wilkinson, A. J., Parkinson, T., Leatherbarrow, R. J., Tate, E. W., Holder, A. A. and Smith, D. F. (2012). Selective Inhibitors of Protozoan Protein *N*-Myristoyltransferases as Starting Points for Tropical Disease Medicinal Chemistry Programs. *PLOS Negl Trop Dis* **6**, e1625. doi:10.1371/journal.pntd.0001625.

Bologna, G., Yvon, C., Duvaud, S. and Veuthey, A.-L. (2004). N-Terminal myristoylation predictions by ensembles of neural networks. *Proteomics* **4**, 1626–1632. doi:10.1002/pmic.200300783.

Boutin, J. A. (1997). Myristoylation. *Cellular Signalling* **9**, 15–35. doi:10.1016/S0898-6568(96)00100-3.

Bowyer, P. W., Gunaratne, R. S., Grainger, M., Withers-Martinez, C., Wickramsinghe, S. R., Tate, E. W., Leatherbarrow, R. J., Brown, K. A., Holder, A. A. and Smith, D. F. (2007). Molecules incorporating a benzothiazole core scaffold inhibit the *N*-myristoyltransferase of *Plasmodium falciparum*. *The Biochemical Journal* **408**, 173–180. doi:10.1042/BJ20070692.

Bowyer, P. W., Tate, E. W., Leatherbarrow, R. J., Holder, A. A., Smith, D. F. and Brown, K. A. (2008). *N*-Myristoyltransferase: a Prospective Drug Target for Protozoan Parasites. *ChemMedChem* **3**, 402–408. doi:10.1002/cmdc.200700301.

Brand, S., Cleghorn, L. A. T., McElroy, S. P., Robinson, D. A., Smith, V. C., Hallyburton, I., Harrison, J. R., Norcross, N. R., Spinks, D., Bayliss, T., Norval, S., Stojanovski, L., Torrie, L. S., Frearson, J. A., Brenk, R., Fairlamb, A. H., Ferguson, M. A. J., Read, K. D., Wyatt, P. G. and Gilbert, I. H. (2012). Discovery of a novel class of orally active trypanocidal *N*-myristoyltransferase inhibitors. *Journal of Medicinal Chemistry* **55**, 140–152. doi:10.1021/jm201091t.

Brand, S., Norcross, N. R., Thompson, S., Harrison, J. R., Smith, V. C., Robinson, D. A., Torrie, L. S., McElroy, S. P., Hallyburton, I., Norval, S., Scullion, P., Stojanovski, L., Simeons, F. R. C., van Aalten, D., Frearson, J. A., Brenk, R., Fairlamb, A. H., Ferguson, M. A. J., Wyatt, P. G., Gilbert, I. H. and Read, K. D. (2014). Lead Optimization of a Pyrazole Sulfonamide Series of *Trypanosoma brucei N*-Myristoyltransferase Inhibitors: Identification and Evaluation of CNS Penetrant Compounds as Potential Treatments for Stage 2 Human African Trypanosomiasis. *Journal of Medicinal Chemistry* **57**, 9855–9869. doi:10.1021/jm500809c.

Brannigan, J. A., Roberts, S. M., Bell, A. S., Hutton, J. A., Hodgkinson, M. R., Tate, E. W., Leatherbarrow, R. J., Smith, D. F. and Wilkinson, A. J. (2014). Diverse modes of binding in structures of *Leishmania major N*-myristoyltransferase with selective inhibitors. *IUCrJ* **1**, 250–260. doi:10.1107/S2052252514013001.

Broncel, M., Serwa, R. A., Ciepla, P., Krause, E., Dallman, M. J., Magee, A. I. and Tate, E. W. (2015). Multifunctional Reagents for Quantitative Proteome-Wide Analysis of Protein Modification in Human Cells and Dynamic Profiling of Protein Lipidation During Vertebrate Development. *Angewandte Chemie International Edition* **54**, 5948–5951. doi:10.1002/anie.201500342.

Caballero, M. C., Alonso, A. M., Deng, B., Attias, M., de Souza, W. and Corvi, M. M. (2016). Identification of new palmitoylated proteins in *Toxoplasma gondii*. *Biochimica Et Biophysica Acta* **1864**, 400–408. doi:10.1016/j.bbapap.2016.01.010.

Child, M. A., Hall, C. I., Beck, J. R., Ofori, L. O., Albrow, V. E., Garland, M., Bowyer, P. W., Bradley, P. J., Powers, J. C., Boothroyd, J. C., Weerapana, E. and Bogyo, M. (2013). Small-molecule inhibition of a depalmitoylase enhances *Toxoplasma* host-cell invasion. *Nature Chemical Biology* **9**, 651–656. doi:10.1038/nchembio.1315.

Coleman, R. A., Rao, P., Fogelsong, R. J. and Bardes, E. S. (1992). 2-Bromopalmitoyl-CoA and 2-bromopalmitate: promiscuous inhibitors of membrane-bound enzymes. *Biochimica Et Biophysica Acta* **1125**, 203–209.

Davda, D., El Azzouny, M. A., Tom, C. T. M. B., Hernandez, J. L., Majmudar, J. D., Kennedy, R. T. and Martin, B. R. (2013). Profiling Targets of the Irreversible Palmitoylation Inhibitor 2-Bromopalmitate. *ACS Chemical Biology* **8**, 1912–1917. doi:10.1021/cb400380s.

Doering, T. L., Lu, T., Werbovetz, K. A., Gokel, G. W., Hart, G. W., Gordon, J. I. and Englund, P. T. (1994). Toxicity of myristic acid analogs toward African trypanosomes. *Proceedings of the National Academy of Sciences* **91**, 9735–9739.

Emmer, B. T., Souther, C., Toriello, K. M., Olson, C. L., Epting, C. L. and Engman, D. M. (2009). Identification of a palmitoyl acyltransferase required for protein sorting to the flagellar membrane. *Journal of Cell Science* **122**, 867–874. doi:10.1242/jcs.041764.

Emmer, B. T., Nakayasu, E. S., Souther, C., Choi, H., Sobreira, T. J. P., Epting, C. L., Nesvizhskii, A. I., Almeida, I. C. and Engman, D. M. (2011). Global Analysis of Protein Palmitoylation in African Trypanosomes. *Eukaryotic Cell* **10**, 455–463. doi:10.1128/EC.00248-10.

Ferguson, M. A., Low, M. G. and Cross, G. A. (1985). Glycosyl-sn-1,2-dimyristylphosphatidylinositol is covalently linked to *Trypanosoma brucei* variant surface glycoprotein. *The Journal of Biological Chemistry* **260**, 14547–14555.

Flegr, J., Prandota, J., Sovičková, M. and Israili, Z. H. (2014). Toxoplasmosis – A Global Threat. Correlation of Latent Toxoplasmosis with Specific Disease Burden in a Set of 88 Countries. *PLoS ONE* **9**,. doi:10.1371/journal.pone.0090203.

Foe, I. T., Child, M. A., Majmudar, J. D., Krishnamurthy, S., van der Linden, W. A., Ward, G. E., Martin, B. R. and Bogyo, M. (2015). Global Analysis of Palmitoylated Proteins in *Toxoplasma gondii*. *Cell Host & Microbe* **18**, 501–511. doi:10.1016/j.chom.2015.09.006.

Forrester, M. T., Hess, D. T., Thompson, J. W., Hultman, R., Moseley, M. A., Stamler, J. S. and Casey, P. J. (2011). Site-specific analysis of protein S-acylation by resin-assisted capture. *Journal of Lipid Research* **52**, 393–398. doi:10.1194/jlr.D011106.

Frearson, J. A., Brand, S., McElroy, S. P., Cleghorn, L. A. T., Smid, O., Stojanovski, L., Price, H. P., Guther, M. L. S., Torrie, L. S., Robinson, D. A., Hallyburton, I., Mpamhanga, C. P., Brannigan, J. A., Wilkinson, A. J., Hodgkinson, M., Hui, R., Qiu, W., Raimi, O. G., van Aalten, D. M. F., Brenk, R., Gilbert, I. H., Read, K. D., Fairlamb, A. H., Ferguson, M. A. J., Smith, D. F. and Wyatt, P. G. (2010). *N*-myristoyltransferase inhibitors as new leads to treat sleeping sickness. *Nature* **464**, 728–732. doi:10.1038/nature08893.

Frénal, K., Tay, C. L., Mueller, C., Bushell, E. S., Jia, Y., Graindorge, A., Billker, O., Rayner, J. C. and Soldati-Favre, D. (2013). Global Analysis of Apicomplexan Protein *S*-Acyl Transferases Reveals

690 an Enzyme Essential for Invasion: Repertoire of Essential PATs in Two Apicomplexans. *Traffic*
691 **14**, 895–911. doi:10.1111/tra.12081.

692 **Galvin, B. D., Li, Z., Villemaine, E., Poole, C. B., Chapman, M. S., Pollastri, M. P., Wyatt, P. G. and**
693 **Carlow, C. K. S.** (2014). A Target Repurposing Approach Identifies *N*-myristoyltransferase as a
694 New Candidate Drug Target in Filarial Nematodes. *PLoS Neglected Tropical Diseases* **8**.
695 doi:10.1371/journal.pntd.0003145.

696 **Godsel, L. M.** (1999). Flagellar protein localization mediated by a calcium-myristoyl/palmitoyl switch
697 mechanism. *The EMBO Journal* **18**, 2057–2065. doi:10.1093/emboj/18.8.2057.

698 **Goldston, A. M., Sharma, A. I., Paul, K. S. and Engman, D. M.** (2014). Acylation in trypanosomatids:
699 an essential process and potential drug target. *Trends in parasitology* **30**, 350–360.
700 doi:10.1016/j.pt.2014.05.003.

701 **Goncalves, V., Brannigan, J. A., Thinon, E., Olaleye, T. O., Serwa, R., Lanzarone, S., Wilkinson, A. J.,**
702 **Tate, E. W. and Leatherbarrow, R. J.** (2012a). A fluorescence-based assay for N-
703 myristoyltransferase activity. *Analytical Biochemistry* **421**, 342–344.
704 doi:10.1016/j.ab.2011.10.013.

705 **Goncalves, V., Brannigan, J. A., Whalley, D., Ansell, K. H., Saxty, B., Holder, A. A., Wilkinson, A. J.,**
706 **Tate, E. W. and Leatherbarrow, R. J.** (2012b). Discovery of *Plasmodium vivax N*-
707 Myristoyltransferase Inhibitors: Screening, Synthesis, and Structural Characterization of their
708 Binding Mode. *Journal of Medicinal Chemistry* **55**, 3578–3582. doi:10.1021/jm300040p.

709 **Graf, F. E., Ludin, P., Arquint, C., Schmidt, R. S., Schaub, N., Kunz Renggli, C., Munday, J. C.,**
710 **Krezdorn, J., Baker, N., Horn, D., Balmer, O., Caccone, A., de Koning, H. P. and Mäser, P.**
711 (2016). Comparative genomics of drug resistance in *Trypanosoma brucei* rhodesiense.
712 *Cellular and molecular life sciences: CMLS* **73**, 3387–3400. doi:10.1007/s00018-016-2173-6.

Gunaratne, R. S., Sajid, M., Ling, I. T., Tripathi, R., Pachebat, J. A. and Holder, A. A. (2000). Characterization of *N*-myristoyltransferase from *Plasmodium falciparum*. *Biochemical Journal* **348**, 459–463. doi:10.1042/bj3480459.

Guttery, D. S., Poulin, B., Ramaprasad, A., Wall, R. J., Ferguson, D. J. P., Brady, D., Patzewitz, E.-M., Whipple, S., Straschil, U., Wright, M. H., Mohamed, A. M. A. H., Radhakrishnan, A., Arold, S. T., Tate, E. W., Holder, A. A., Wickstead, B., Pain, A. and Tewari, R. (2014). Genome-wide functional analysis of *Plasmodium* protein phosphatases reveals key regulators of parasite development and differentiation. *Cell Host & Microbe* **16**, 128–140. doi:10.1016/j.chom.2014.05.020.

Hajjaran, H., Kazemi-Rad, E., Mohebali, M., Oshaghi, M. A., Khadem-Erfan, M. B., Hajaliloo, E., Reisi Nafchi, H. and Raoofian, R. (2016). Expression analysis of activated protein kinase C gene (LACK1) in antimony sensitive and resistant *Leishmania tropica* clinical isolates using real-time RT-PCR. *International Journal of Dermatology* **55**, 1020–1026. doi:10.1111/ijd.13321.

Heal, W. P., Wickramasinghe, S. R., Leatherbarrow, R. J. and Tate, E. W. (2008). *N*-Myristoyl transferase-mediated protein labelling *in vivo*. *Organic & Biomolecular Chemistry* **6**, 2308–2315. doi:10.1039/B803258K.

Herrera, L. J., Brand, S., Santos, A., Nohara, L. L., Harrison, J., Norcross, N. R., Thompson, S., Smith, V., Lema, C., Varela-Ramirez, A., Gilbert, I. H., Almeida, I. C. and Maldonado, R. A. (2016). Validation of *N*-myristoyltransferase as Potential Chemotherapeutic Target in Mammal-Dwelling Stages of *Trypanosoma cruzi*. *PLoS Neglected Tropical Diseases* **10**. doi:10.1371/journal.pntd.0004540.

Hopp, C. S., Balaban, A. E., Bushell, E. S. C., Billker, O., Rayner, J. C. and Sinnis, P. (2016). Palmitoyl transferases have critical roles in the development of mosquito and liver stages of

Plasmodium: Palmitoyl transferases and mosquito stages of *Plasmodium*. *Cellular Microbiology* **18**, 1625–1641. doi:10.1111/cmi.12601.

Hutton, J. A., Goncalves, V., Brannigan, J. A., Paape, D., Wright, M. H., Waugh, T. M., Roberts, S. M., Bell, A. S., Wilkinson, A. J., Smith, D. F., Leatherbarrow, R. J. and Tate, E. W. (2014). Structure-Based Design of Potent and Selective *Leishmania N*-Myristoyltransferase Inhibitors. *Journal of Medicinal Chemistry* **57**, 8664–8670. doi:10.1021/jm5011397.

Jones, M. L., Collins, M. O., Goulding, D., Choudhary, J. S. and Rayner, J. C. (2012). Analysis of protein palmitoylation reveals a pervasive role in *Plasmodium* development and pathogenesis. *Cell Host & Microbe* **12**, 246–258. doi:10.1016/j.chom.2012.06.005.

Jones, J. L., Parise, M. E. and Fiore, A. E. (2014). Neglected Parasitic Infections in the United States: Toxoplasmosis. *The American Journal of Tropical Medicine and Hygiene* **90**, 794–799. doi:10.4269/ajtmh.13-0722.

Kemp, L. E., Rusch, M., Adibekian, A., Bullen, H. E., Graindorge, A., Freymond, C., Rottmann, M., Braun-Breton, C., Baumeister, S., Porfetye, A. T., Vetter, I. R., Hedberg, C. and Soldati-Favre, D. (2013). Characterization of a Serine Hydrolase Targeted by Acyl-protein Thioesterase Inhibitors in *Toxoplasma gondii*. *The Journal of Biological Chemistry* **288**, 27002–27018. doi:10.1074/jbc.M113.460709.

Keserü, G. M. and Makara, G. M. (2009). The influence of lead discovery strategies on the properties of drug candidates. *Nature Reviews Drug Discovery* **8**, 203–212. doi:10.1038/nrd2796.

Leber, W., Skippen, A., Fivelman, Q. L., Bowyer, P. W., Cockcroft, S. and Baker, D. A. (2009). A unique phosphatidylinositol 4-phosphate 5-kinase is activated by ADP-ribosylation factor in *Plasmodium falciparum*. *International Journal for Parasitology* **39**, 645–653. doi:10.1016/j.ijpara.2008.11.015.

Li, Y. F. and Radivojac, P. (2012). Computational approaches to protein inference in shotgun proteomics. *BMC bioinformatics* **13 Suppl 16**, S4. doi:10.1186/1471-2105-13-S16-S4.

Maurer-Stroh, S., Eisenhaber, B. and Eisenhaber, F. (2002). N-terminal *N*-myristoylation of proteins: prediction of substrate proteins from amino acid sequence. *Journal of Molecular Biology* **317**, 541–557. doi:10.1006/jmbi.2002.5426.

Mbengue, A., Bhattacharjee, S., Pandharkar, T., Liu, H., Estiu, G., Stahelin, R. V., Rizk, S. S., Njimoh, D. L., Ryan, Y., Chotivanich, K., Nguon, C., Ghorbal, M., Lopez-Rubio, J.-J., Pfrender, M., Emrich, S., Mohandas, N., Dondorp, A. M., Wiest, O. and Haldar, K. (2015). A molecular mechanism of artemisinin resistance in *Plasmodium falciparum* malaria. *Nature* **520**, 683–687. doi:10.1038/nature14412.

Mills, E., Price, H. P., Johner, A., Emerson, J. E. and Smith, D. F. (2007). Kinetoplastid PPEF phosphatases: dual acylated proteins expressed in the endomembrane system of *Leishmania*. *Molecular and Biochemical Parasitology* **152**, 22–34. doi:10.1016/j.molbiopara.2006.11.008.

Möskes, C., Burghaus, P. A., Wernli, B., Sauder, U., Dürrenberger, M. and Kappes, B. (2004). Export of *Plasmodium falciparum* calcium-dependent protein kinase 1 to the parasitophorous vacuole is dependent on three N-terminal membrane anchor motifs. *Molecular Microbiology* **54**, 676–691. doi:10.1111/j.1365-2958.2004.04313.x.

Olaleye, T. O., Brannigan, J. A., Roberts, S. M., Leatherbarrow, R. J., Wilkinson, A. J. and Tate, E. W. (2014). Peptidomimetic inhibitors of *N*-myristoyltransferase from human malaria and leishmaniasis parasites. *Organic & Biomolecular Chemistry* **12**, 8132–8137. doi:10.1039/c4ob01669f.

Paape, D., Bell, A. S., Heal, W. P., Hutton, J. A., Leatherbarrow, R. J., Tate, E. W. and Smith, D. F. (2014). Using a Non-Image-Based Medium-Throughput Assay for Screening Compounds

783 Targeting *N*-myristoylation in Intracellular *Leishmania* Amastigotes. *PLoS Neglected Tropical*
784 *Diseases* **8**. doi:10.1371/journal.pntd.0003363.

785 **Percher, A., Ramakrishnan, S., Thinon, E., Yuan, X., Yount, J. S. and Hang, H. C.** (2016). Mass-tag
786 labeling reveals site-specific and endogenous levels of protein *S*-fatty acylation. *Proceedings*
787 *of the National Academy of Sciences of the United States of America* **113**, 4302–4307.
788 doi:10.1073/pnas.1602244113.

789 **Poulin, B., Patzewitz, E.-M., Brady, D., Silvie, O., Wright, M. H., Ferguson, D. J. P., Wall, R. J.,**
790 **Whipple, S., Guttery, D. S., Tate, E. W., Wickstead, B., Holder, A. A. and Tewari, R.** (2013).
791 Unique apicomplexan IMC sub-compartment proteins are early markers for apical polarity in
792 the malaria parasite. *Biology Open* **2**, 1160–1170. doi:10.1242/bio.20136163.

793 **Price, H. P., Menon, M. R., Panethymitaki, C., Goulding, D., McKean, P. G. and Smith, D. F.** (2003).
794 Myristoyl-CoA:protein *N*-myristoyltransferase, an essential enzyme and potential drug target
795 in kinetoplastid parasites. *The Journal of Biological Chemistry* **278**, 7206–7214.
796 doi:10.1074/jbc.M211391200.

797 **Price, H. P., Hodgkinson, M. R., Wright, M. H., Tate, E. W., Smith, B. A., Carrington, M., Stark, M.**
798 **and Smith, D. F.** (2012). A role for the vesicle-associated tubulin binding protein ARL6 (BBS3)
799 in flagellum extension in *Trypanosoma brucei*. *Biochimica Et Biophysica Acta* **1823**, 1178–
800 1191. doi:10.1016/j.bbamcr.2012.05.007.

801 **Proto, W. R., Castanys-Munoz, E., Black, A., Tetley, L., Moss, C. X., Juliano, L., Coombs, G. H. and**
802 **Mottram, J. C.** (2011). *Trypanosoma brucei* Metacaspase 4 Is a Pseudopeptidase and a
803 Virulence Factor. *Journal of Biological Chemistry* **286**, 39914–39925.
804 doi:10.1074/jbc.M111.292334.

805 **Rackham, M. D., Brannigan, J. A., Moss, D. K., Yu, Z., Wilkinson, A. J., Holder, A. A., Tate, E. W. and**
806 **Leatherbarrow, R. J.** (2013). Discovery of Novel and Ligand-Efficient Inhibitors of *Plasmodium*

falciparum and *Plasmodium vivax N*-Myristoyltransferase. *Journal of Medicinal Chemistry* **56**, 371–375. doi:10.1021/jm301474t.

Rackham, M. D., Brannigan, J. A., Rangachari, K., Meister, S., Wilkinson, A. J., Holder, A. A., Leatherbarrow, R. J. and Tate, E. W. (2014). Design and Synthesis of High Affinity Inhibitors of *Plasmodium falciparum* and *Plasmodium vivax N*-Myristoyltransferases Directed by Ligand Efficiency Dependent Lipophilicity (LELP). *Journal of Medicinal Chemistry* **57**, 2773–2788. doi:10.1021/jm500066b.

Rackham, M. D., Yu, Z., Brannigan, J. A., Heal, W. P., Paape, D., Barker, K. V., Wilkinson, A. J., Smith, D. F., Leatherbarrow, R. J. and Tate, E. W. (2015). Discovery of high affinity inhibitors of *Leishmania donovani N*-myristoyltransferase. *MedChemComm* **6**, 1761–1766. doi:10.1039/c5md00241a.

Rahlfs, S., Koncarevic, S., Iozef, R., Mailu, B. M., Savvides, S. N., Schirmer, R. H. and Becker, K. (2009). Myristoylated adenylate kinase-2 of *Plasmodium falciparum* forms a heterodimer with myristoyltransferase. *Molecular and Biochemical Parasitology* **163**, 77–84. doi:10.1016/j.molbiopara.2008.09.008.

Rees-Channer, R. R., Martin, S. R., Green, J. L., Bowyer, P. W., Grainger, M., Molloy, J. E. and Holder, A. A. (2006). Dual acylation of the 45 kDa gliding-associated protein (GAP45) in *Plasmodium falciparum* merozoites. *Molecular and Biochemical Parasitology* **149**, 113–116. doi:10.1016/j.molbiopara.2006.04.008.

Ren, J., Wen, L., Gao, X., Jin, C., Xue, Y. and Yao, X. (2008). CSS-Palm 2.0: an updated software for palmitoylation sites prediction. *Protein engineering, design & selection: PEDS* **21**, 639–644. doi:10.1093/protein/gzn039.

Resh, M. D. (1999). Fatty acylation of proteins: new insights into membrane targeting of myristoylated and palmitoylated proteins. *Biochimica et Biophysica Acta (BBA) - Molecular Cell Research* **1451**, 1–16. doi:10.1016/S0167-4889(99)00075-0.

Resh, M. D. (2006). Trafficking and signaling by fatty-acylated and prenylated proteins. *Nature Chemical Biology* **2**, 584–590. doi:10.1038/nchembio834.

Resh, M. D. (2016). Fatty acylation of proteins: The long and the short of it. *Progress in Lipid Research* **63**, 120–131. doi:10.1016/j.plipres.2016.05.002.

Roberts, A. J. and Fairlamb, A. H. (2016). The *N*-myristoylome of *Trypanosoma cruzi*. *Scientific Reports* **6**, 31078. doi:10.1038/srep31078.

Roberts, A. J., Torrie, L. S., Wyllie, S. and Fairlamb, A. H. (2014). Biochemical and genetic characterization of *Trypanosoma cruzi N*-myristoyltransferase. *The Biochemical Journal* **459**, 323–332. doi:10.1042/BJ20131033.

Roth, A. F., Wan, J., Bailey, A. O., Sun, B., Kuchar, J. A., Green, W. N., Phinney, B. S., Yates, J. R. and Davis, N. G. (2006). Global analysis of protein palmitoylation in yeast. *Cell* **125**, 1003–1013. doi:10.1016/j.cell.2006.03.042.

Sádlová, J., Price, H. P., Smith, B. A., Votýpka, J., Volf, P. and Smith, D. F. (2010). The stage-regulated HASPB and SHERP proteins are essential for differentiation of the protozoan parasite *Leishmania major* in its sand fly vector, *Phlebotomus papatasi*. *Cellular Microbiology* **12**, 1765–1779. doi:10.1111/j.1462-5822.2010.01507.x.

Sahin, A., Espiau, B., Tetaud, E., Cuvillier, A., Lartigue, L., Ambit, A., Robinson, D. R. and Merlin, G. (2008). The *Leishmania* ARL-1 and Golgi Traffic. *PLOS ONE* **3**, e1620. doi:10.1371/journal.pone.0001620.

Santos, J. M., Duarte, N., Kehrer, J., Ramesar, J., Avramut, M. C., Koster, A. J., Dessens, J. T., Frischknecht, F., Chevalley-Maurel, S., Janse, C. J., Franke-Fayard, B. and Mair, G. R. (2016). Maternally supplied *S*-acyl-transferase is required for crystalloid organelle formation and transmission of the malaria parasite. *Proceedings of the National Academy of Sciences* **113**, 7183–7188. doi:10.1073/pnas.1522381113.

Sinha, S., Medhi, B. and Sehgal, R. (2014). Challenges of drug-resistant malaria. *Parasite* **21**,. doi:10.1051/parasite/2014059.

Spinks, D., Smith, V., Thompson, S., Robinson, D. A., Luksch, T., Smith, A., Torrie, L. S., McElroy, S., Stojanovski, L., Norval, S., Collie, I. T., Hallyburton, I., Rao, B., Brand, S., Brenk, R., Frearson, J. A., Read, K. D., Wyatt, P. G. and Gilbert, I. H. (2015). Development of Small-Molecule *Trypanosoma brucei N*-Myristoyltransferase Inhibitors: Discovery and Optimisation of a Novel Binding Mode. *Chemmedchem* **10**, 1821–1836. doi:10.1002/cmdc.201500301.

Tate, E. W., Bell, A. S., Rackham, M. D. and Wright, M. H. (2014). *N*-Myristoyltransferase as a potential drug target in malaria and leishmaniasis. *Parasitology* **141**, 37–49. doi:10.1017/S0031182013000450.

Tate, E. W., Kalesh, K. A., Lanyon-Hogg, T., Storck, E. M. and Thinon, E. (2015). Global profiling of protein lipidation using chemical proteomic technologies. *Current Opinion in Chemical Biology* **24**, 48–57. doi:10.1016/j.cbpa.2014.10.016.

Tay, C. L., Jones, M. L., Hodson, N., Theron, M., Choudhary, J. S. and Rayner, J. C. (2016). Study of *Plasmodium falciparum* DHHC palmitoyl transferases identifies a role for PfDHHC9 in gametocytogenesis: Study of *Plasmodium falciparum* DHHC palmitoyl transferases. *Cellular Microbiology* **18**, 1596–1610. doi:10.1111/cmi.12599.

WHO (2015). World Malaria Report 2015.

WHO (2016a). Leishmaniasis Fact Sheet.

WHO (2016b). Trypanosomiasis Fact Sheet.

Wilcox, C., Hu, J. S. and Olson, E. N. (1987). Acylation of proteins with myristic acid occurs cotranslationally. *Science* **238**, 1275–1278. doi:10.1126/science.3685978.

Wright, M. H., Heal, W. P., Mann, D. J. and Tate, E. W. (2009). Protein myristoylation in health and disease. *Journal of Chemical Biology* **3**, 19–35. doi:10.1007/s12154-009-0032-8.

Wright, M. H., Clough, B., Rackham, M. D., Rangachari, K., Brannigan, J. A., Grainger, M., Moss, D. K., Bottrill, A. R., Heal, W. P., Broncel, M., Serwa, R. A., Brady, D., Mann, D. J., Leatherbarrow, R. J., Tewari, R., Wilkinson, A. J., Holder, A. A. and Tate, E. W. (2014). Validation of *N*-myristoyltransferase as an antimalarial drug target using an integrated chemical biology approach. *Nature chemistry* **6**, 112–121. doi:10.1038/nchem.1830.

Wright, M. H., Paape, D., Storck, E. M., Serwa, R. A., Smith, D. F. and Tate, E. W. (2015). Global Analysis of Protein *N*-Myristoylation and Exploration of *N*-Myristoyltransferase as a Drug Target in the Neglected Human Pathogen *Leishmania donovani*. *Chemistry & Biology* **22**, 342–354. doi:10.1016/j.chembiol.2015.01.003.

Wright, M. H., Paape, D., Price, H. P., Smith, D. F. and Tate, E. W. (2016). Global Profiling and Inhibition of Protein Lipidation in Vector and Host Stages of the Sleeping Sickness Parasite *Trypanosoma brucei*. *ACS Infectious Diseases* **2**, 427–441. doi:10.1021/acsinfecdis.6b00034.

Yu, Z., Brannigan, J. A., Moss, D. K., Brzozowski, A. M., Wilkinson, A. J., Holder, A. A., Tate, E. W. and Leatherbarrow, R. J. (2012). Design and Synthesis of Inhibitors of *Plasmodium falciparum N*-Myristoyltransferase, A Promising Target for Antimalarial Drug Discovery. *Journal of Medicinal Chemistry* **55**, 8879–8890. doi:10.1021/jm301160h.

Yu, Z., Brannigan, J. A., Rangachari, K., Heal, W. P., Wilkinson, A. J., Holder, A. A., Leatherbarrow, R. J. and Tate, E. W. (2015). Discovery of pyridyl-based inhibitors of *Plasmodium falciparum* N-myristoyltransferase. *MedChemComm* **6**, 1767–1772. doi:10.1039/c5md00242g.

Zheng, B., DeRan, M., Li, X., Liao, X., Fukata, M. and Wu, X. (2013). 2-Bromopalmitate Analogues as Activity-Based Probes To Explore Palmitoyl Acyltransferases. *Journal of the American Chemical Society* **135**, 7082–7085. doi:10.1021/ja311416v.

Figure 1. Workflow of the acyl biotin exchange (ABE) approach to identify *S*-acylated proteins. Free thiols in protein lysates are blocked with *N*-ethyl maleimide followed by selective cleavage of thioesters using hydroxylamine and labelling of the liberated thiols with HPDP-biotin. Next, a typical proteomics workflow that includes affinity enrichment of the biotinylated proteins, proteolytic digest, and analysis of the peptide fragments by mass spectrometry enables the identification of *S*-acylated proteins. A control sample that still contains the intact thioesters and therefore no biotin tags facilitates the identification of non-specifically enriched proteins.

Figure 2. A) Workflow of 'metabolic tagging with click chemistry' (MTCC) approach. Analogues of the investigated PTM (e.g. compounds shown in **B**) are fed to cells and incorporated into the corresponding proteins. After cell lysis, an affinity tag is attached to the analogue using bio-orthogonal CuAAC. Affinity enrichment followed by tryptic digestion and analysis of the peptide fragments by mass spectrometry facilitates the identification of proteins that exhibit this specific PTM. **B)** Myristic and palmitic acid probes that have been applied in an MTCC approach in protozoan parasites.

Figure 3. A) Comparison of *P. falciparum* proteins identified via ABE and MTCC (with 17-ODYA (**4**); workflows: cf. **Fig. 1** and **2A**) techniques in the study of Jones *et al.* **B)** Comparison of *T. gondii* proteins identified in the studies of Caballero *et al.* and Foe *et al.*. which used a complementary ABE approach (cf. **Fig. 1**) and a global analysis of 17-ODYA (**4**) tagged proteins in the presence and absence of hydroxylamine, respectively. Total rather than high confidence hits were used in each case. **C)** Comparison of the 321 putative *P. falciparum* palmitoyl proteins (from Jones *et al.*, 2012) that have *T. gondii* orthologues with putative *T. gondii* palmitoyl proteins (Caballero *et al.*, 2016; *Foe et al*, 2015). **D)** Likely dual acylated proteins in *P. falciparum*. (**Supplementary Table S1**). Numbers in the Venn diagrams may differ slightly from those reported in the primary literature due to revisions in sequence databases over time, ID mapping issues (e.g. between the two *Tg* species analysed in **B**), and, in diagram **C**, the manner in which the protein inference problem has been handled; most proteomic analyses group proteins when they cannot be distinguished by mass spectrometry, but here each protein was treated independently.

Figure 4. A) YnMyr-CoA crystallised in the Myr-CoA binding pocket of *Pv*NMT (PDB: 2YNC). **B)** YnMyr (**1**) is incorporated into proteins via both amide (NaOH-insensitive) and ester (NaOH-sensitive) linkages. Proteomics revealed the base-sensitive incorporation to be on GPI anchored proteins. **C)** Dose-response of YnMyr (**1**) incorporation upon co-incubation with NMT inhibitor DDD85646 (**19**). In-gel fluorescence read-out (graph on the right: quantification of fluorescence intensity) following the workflow shown in **Fig. 2A** and includinga base-treatment step to remove GPI anchor labelling. Figure adapted from: (Wright *et al.*, 2014).

Figure 5. A) Comparison of MTCC (workflow: **Fig. 2A**) with palmitate analogue YnPal (**2**) and myristate analogue YnMyr (**1**) in bloodstream form (BSF) *T. brucei*. **B)** In-gel fluorescence read-out of the effect of NMT inhibition with DDD85646 (**19**) on YnMyr (**1**) labelling in BSF parasites. YnMyr (**1**) incorporation into GPI anchored proteins, such as the VSG (Variant Surface Glycoprotein; indicated by arrow), is unaffected but incorporation into *N*-myristoylated proteins drops. Figure adapted from (Wright *et al.*, 2016).

Figure 6. A) Comparison of *T. brucei* proteins identified via ABE and MTCC (with YnMyr (**1**); workflows: **Fig. 1** and **2A**) techniques in the studies of Emmer *et al.* and Wright *et al.* **B)** Comparison of high confidence *T. brucei* myristoyl proteins that have *T. cruzi* orthologues with high confidence *T. cruzi* myristoyl proteins. **C)** Comparison of high confidence *T. brucei* myristoyl proteins that have *L. donovani* orthologues with high confidence *L. donovani* myristoyl proteins. Numbers in the Venn diagrams may differ slightly from those reported in the primary literature due to revision of sequence

databases over time and, in **B** and **C**, the manner in which the protein inference problem has been handled (see Fig. 3). **D)** Candidate dual acylated proteins in *T. brucei* (high confidence NMT substrates also identified by both palmitoyl proteome studies (Emmer *et al.*, 2011; Wright *et al.*, 2016). **E)** High confidence *N*-myristoyl proteins conserved across all three organisms. (**Supplementary Table S2**).

Figure 7. Studying protein *N*-myristoylation in *Leishmania* parasites. YnMyr (**1**) was incubated with parasites, in some cases in the presence of NMT inhibitors **19** or **19a**. Following incorporation into proteins, click chemistry was used to append a fluorophore or affinity handle; in-gel fluorescence analysis (**A**) provided a simple read-out for inhibitor activity in cells, and quantitative chemical proteomics (**B**) enabled the identification of proteins and lipidation sites. This study also compared different life stages of the parasite: promastigotes (Pro.) and amastigotes (Am.). MG = protein contains an N-terminal glycine (possible NMT substrate). Figure adapted from (Wright *et al.*, 2015).

Figure 8. A) Superposition of the crystal structures of the quinoline (**5**) and the 1,2,4-oxadiazole (**16**) based inhibitors in complex with *Pv*NMT (PDB code: 4A95, compound **5**, orange; 4B14, compound **16**, blue) and biological activity of the quinoline compounds **5** and **6** against *Pv*NMT, *Hs*NMT1, and *Hs*NMT2 (Yu *et al.*, 2015). **B)** Superposition of the crystal structures of aminoacylpyrrolidine **7**, piperidinylindole **8**, and the corresponding hybridization product **9** in complex with *Ld*NMT (PDB code: 4cgl, compound **7**, green; 4cgn, compound **8**, blue; 4cyo, compound **9**, red) and biological activity of **7**, **8**, and **9** against *Ld*NMT, *Hs*NMT1, and antiparasitic activity against extracellular amastigotes of *L. donovani* (Hutton *et al.*, 2014). The piperidinylindole **8** and the hybridization product **9** show an interaction of a basic centre with the C-terminal carboxylate of NMT. Additionally, all compounds show interactions with a set of aromatic amino acids.

Figure 9. A) Biological activity against *Pf*NMT and *Hs*NMT1 and antiparasitic activity against *P. falciparum* 3D7 of NMT inhibitors derived from R0-09-4609 (**10**) by scaffold-hopping. The superposition of the crystal structures of the benzo[*b*]furan based derivative **12** and the scaffold simplified analogue **16** in complex with *Pv*NMT indicates competitive binding of the inhibitors with the peptide substrate (PDB code: 4UFV, compound **12**, orange; 4B14, compound **16**, blue) (Yu *et al.*, 2015). **B)** Crystal structure of the *N*-myristoylated inhibitor product in complex with *Pv*NMT. The peptidomimetic inhibitor (**18**) is shown in orange and the myristic acid moiety in blue (Pdb code: 4c7h). Additionally, 20% of the electron density corresponds to the CoA by-product (in red), providing structural evidence for a product complex in NMT for the first time (Olaleye *et al.*, 2014).

Figure 10. A) Biological activity against *Tb*NMT and *Hs*NMT1, antiparasitic cell activity against bloodstream form *T. brucei* parasites, and BBB permeability (B:B = brain to blood ratio, ND = not determined) of *Tb*NMT lead inhibitors (Brand *et al.*, 2014; Spinks *et al.*, 2015). **B)** Superpositions of the crystal structures of DDD85646 (**19**) (PDB code: 2WSA, red) with, respectively, lead compounds of the thiazolidinone (**21**) (PDB code: 5AG6, green) and benzomorpholinone (**22**) (PDB code: 5AGE, blue) series in complex with the *Tb*NMT surrogate *Lm*NMT reveal that the two new inhibitor classes (**21** and **22**) exhibit a different binding mode than the sulphonamides (**19**) (Spinks *et al.*, 2015).

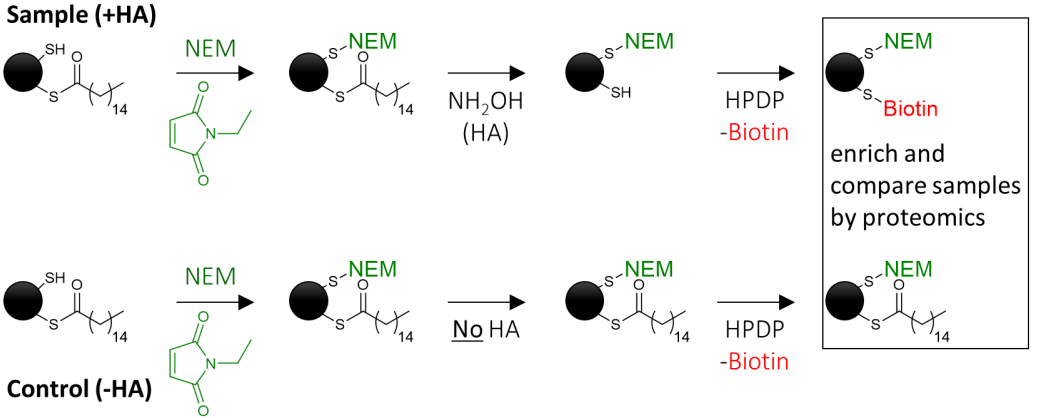
Sample (+HA)
NEM
NEM
NH2OH
(HA)
NEM
HPDP
-Biotin
NEM
Biotin
enrich and
compare samples
by proteomics
NEM
NEM
No HA
NEM
HPDP
-Biotin
NEM
Control (-HA)

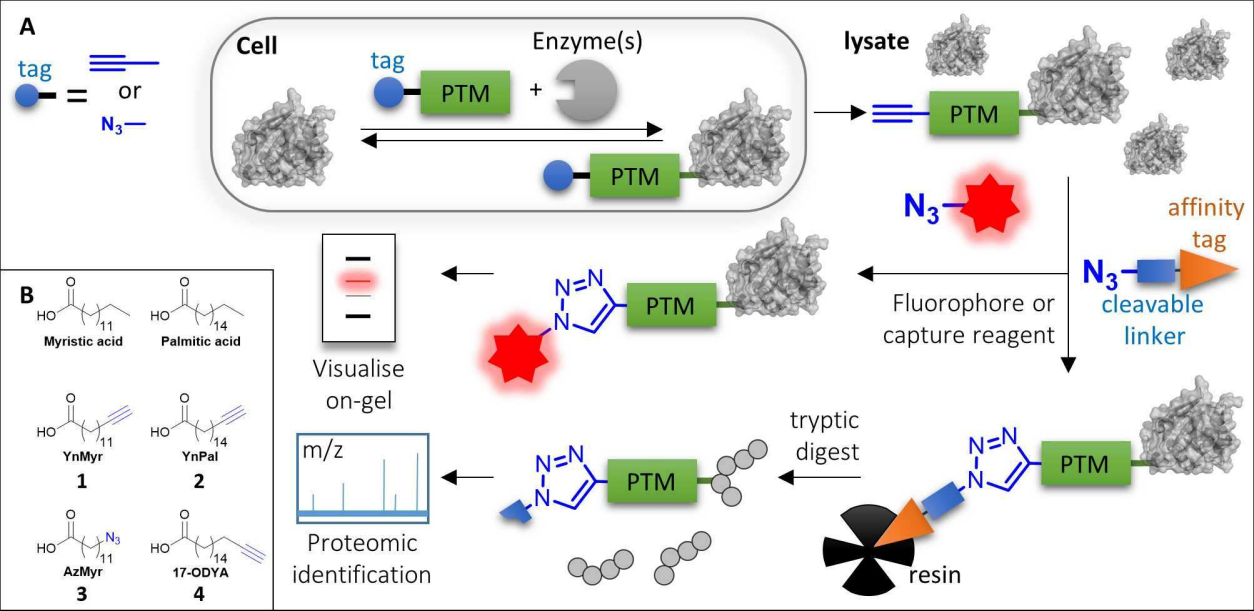
A
tag
=
or
N_3
Cell
tag
PTM
+
Enzyme(s)
PTM
lysate
PTM
N_3
affinity tag
N_3
cleavable linker
Fluorophore or capture reagent
PTM
PTM
Visualise on-gel
tryptic digest
PTM
resin
m/z
PTM
Proteomic identification
B
Myristic acid
Palmitic acid
YnMyr
1
YnPal
2
AzMyr
3
17-ODYA
4

A ***Pf*** **palmitoyl proteome (Jones *et al.*, SILAC)**

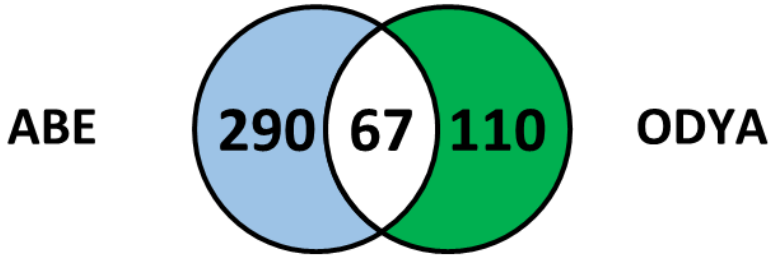

B ***T. gondii*** **palmitoyl proteome**

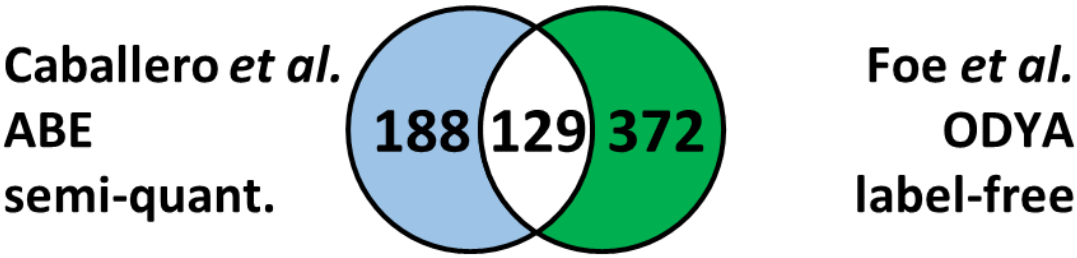

C ***Pf*** **vs** ***Tg*** **palmitome**

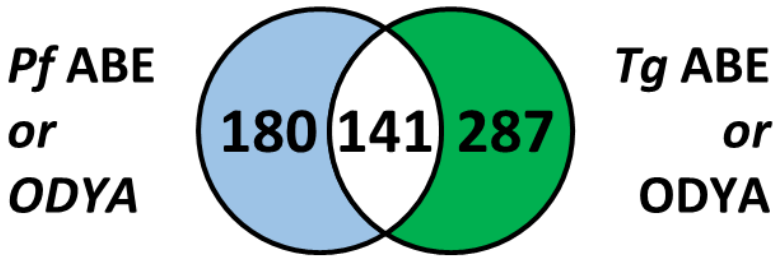

D

Protein ID	Protein name
PF3D7_0217500	CDPK1
PF3D7_0810300	protein phosphatase PPM5
PF3D7_0816200	VPS2
PF3D7_1011000	IMC protein 1
PF3D7_1020900	ADP-ribosylation factor
PF3D7_1137300	CLPTM1 domain-containing
PF3D7_1222700	GAP45
PF3D7_1237700	conserved protein
PF3D7_1310600	Rab-5B
PF3D7_1460600	IMC protein 3

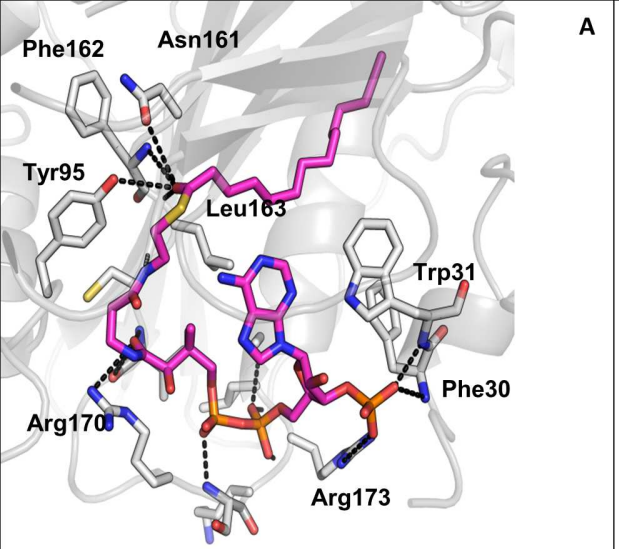
A
Phe162
Asn161
Tyr95
Leu163
Trp31
Phe30
Arg170
Arg173

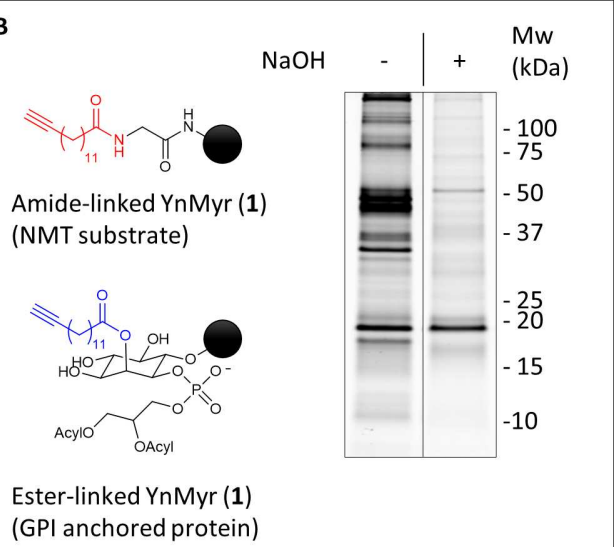
B
NaOH
-
+
Mw
(kDa)
100
75
50
37
25
20
15
10
Amide-linked YnMyr (1)
(NMT substrate)
Ester-linked YnMyr (1)
(GPI anchored protein)

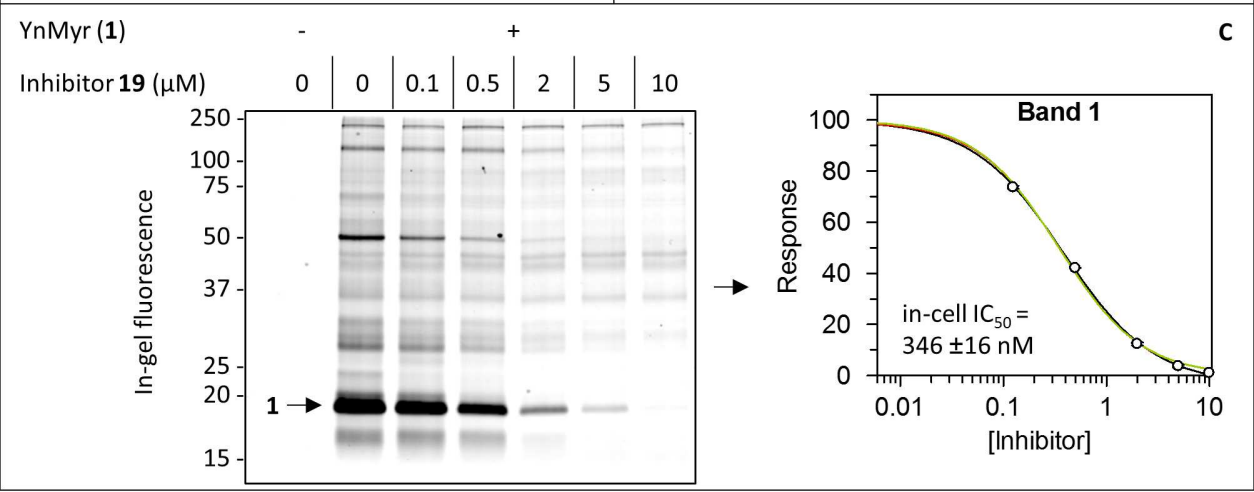
YnMyr (1)
-
+
Inhibitor 19 (μM)
0
0
0.1
0.5
2
5
10
In-gel fluorescence
250
100
75
50
37
25
20
15
1
C
Band 1
Response
100
80
60
40
20
0
in-cell IC50 =
346 ±16 nM
0.01
0.1
1
10
[Inhibitor]

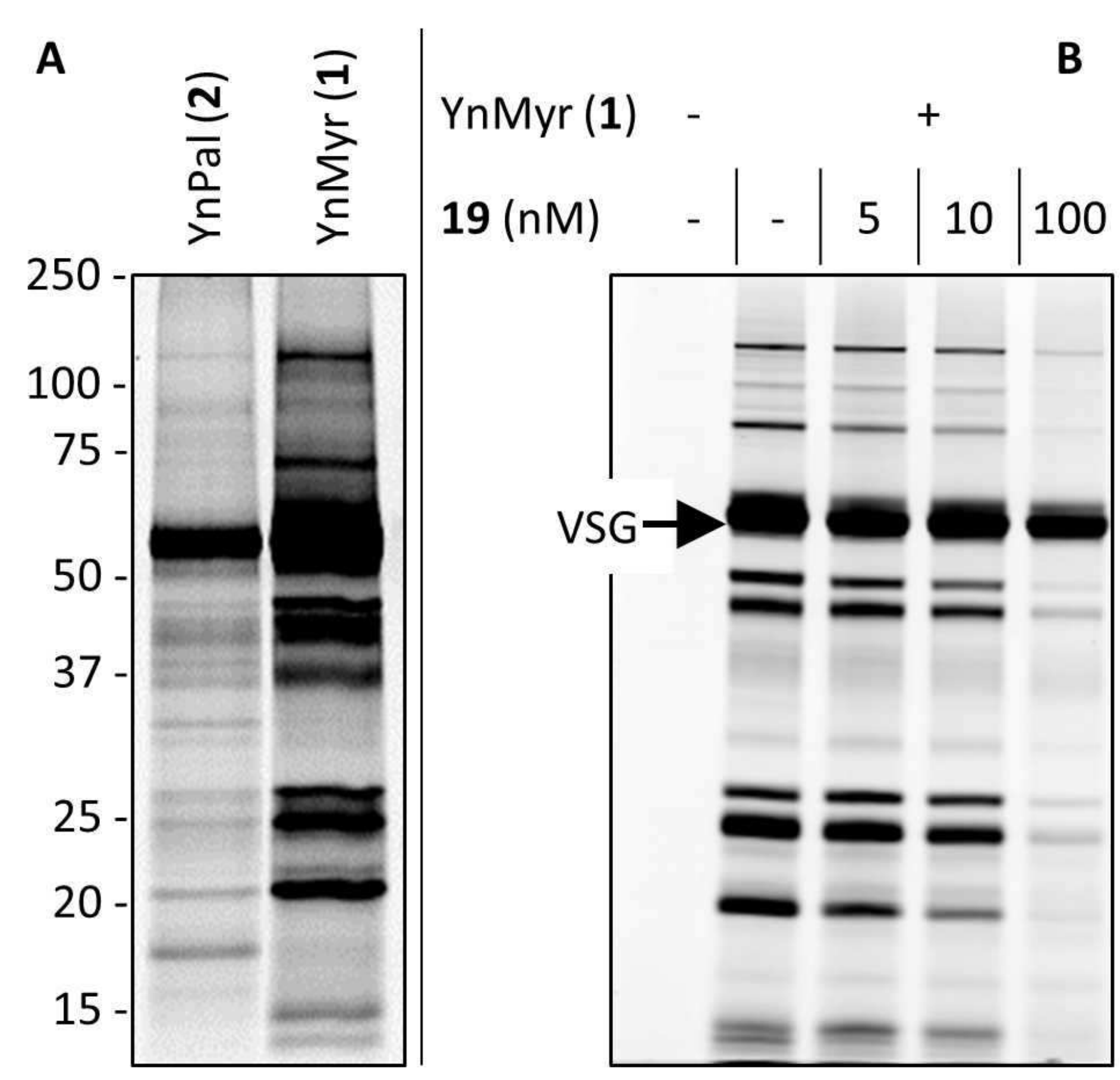
A
YnPal (2)
YnMyr (1)
250
100
75
50
37
25
20
15
B
YnMyr (1) - +
19 (nM) - - 5 10 100
VSG

A Palmitoylation *T. brucei*

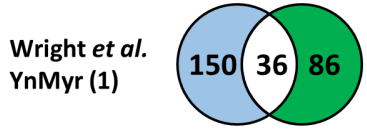

B Myristoylation *T. brucei* vs *T. cruzi*

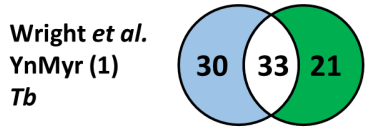

C Myristoylation *T. brucei* vs *L. donovani*

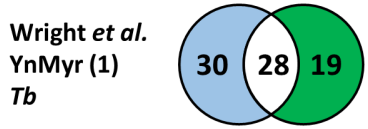

D

Protein ID	Protein name
Tb927.10.2440	Metacaspase-4
Tb927.8.5460	FCaBP-44
Tb927.8.5465	calflagin
Tb927.8.5470	FCaBP-24
Tb927.8.8020	monoglyceride lipase
Tb927.8.8330	calpain, putative
Tb927.1.2120	CALP1.3
Tb927.1.2230	SMP1-1
Tb927.1.4050	ser/thr protein phosphatase
Tb927.10.3260	LACS5
Tb927.4.4360	monoglyceride lipase
Tb927.6.2090	pdz domain protein
Tb927.9.4210	fatty acyl CoA synthetase 3

E

Protein name	*T. brucei* ID	*T. cruzi* ID	*L. donovani* ID
ARF	Tb927.7.6230	TcCLB.508919.60	LdBPK_170080.1
proteasome subunit	Tb927.11.3740	TcCLB.511859.180	LdBPK_130990.1
zinc finger protein	Tb927.10.12940	TcCLB.503939.120	LdBPK_181160.1
conserved protein	Tb927.1.1500	TcCLB.504209.10	LdBPK_200770.1
small myristoylated protein 1 (-1 and -2)	Tb927.1.2230; Tb927.1.2260	TcCLB.509003.30; TcCLB.509003.40	LdBPK_201350.1
AMPK subunit beta	Tb927.8.2450	TcCLB.509331.90	LdBPK_230530.1
protein phosphatase 2C	Tb927.11.760	TcCLB.506925.150	LdBPK_250780.1
uncharacterised protein	Tb927.7.1630; Tb927.8.7760	TcCLB.511389.50	LdBPK_311530.1
ADP-ribosylation factor (ARF)	Tb927.9.13650; Tb927.9.13680 etc	TcCLB.508415.40; TcCLB.508415.50	LdBPK_312890.1
protein phosphatase 2C	Tb927.10.4930	TcCLB.510291.30	LdBPK_321770.1; LdBPK_360560.1

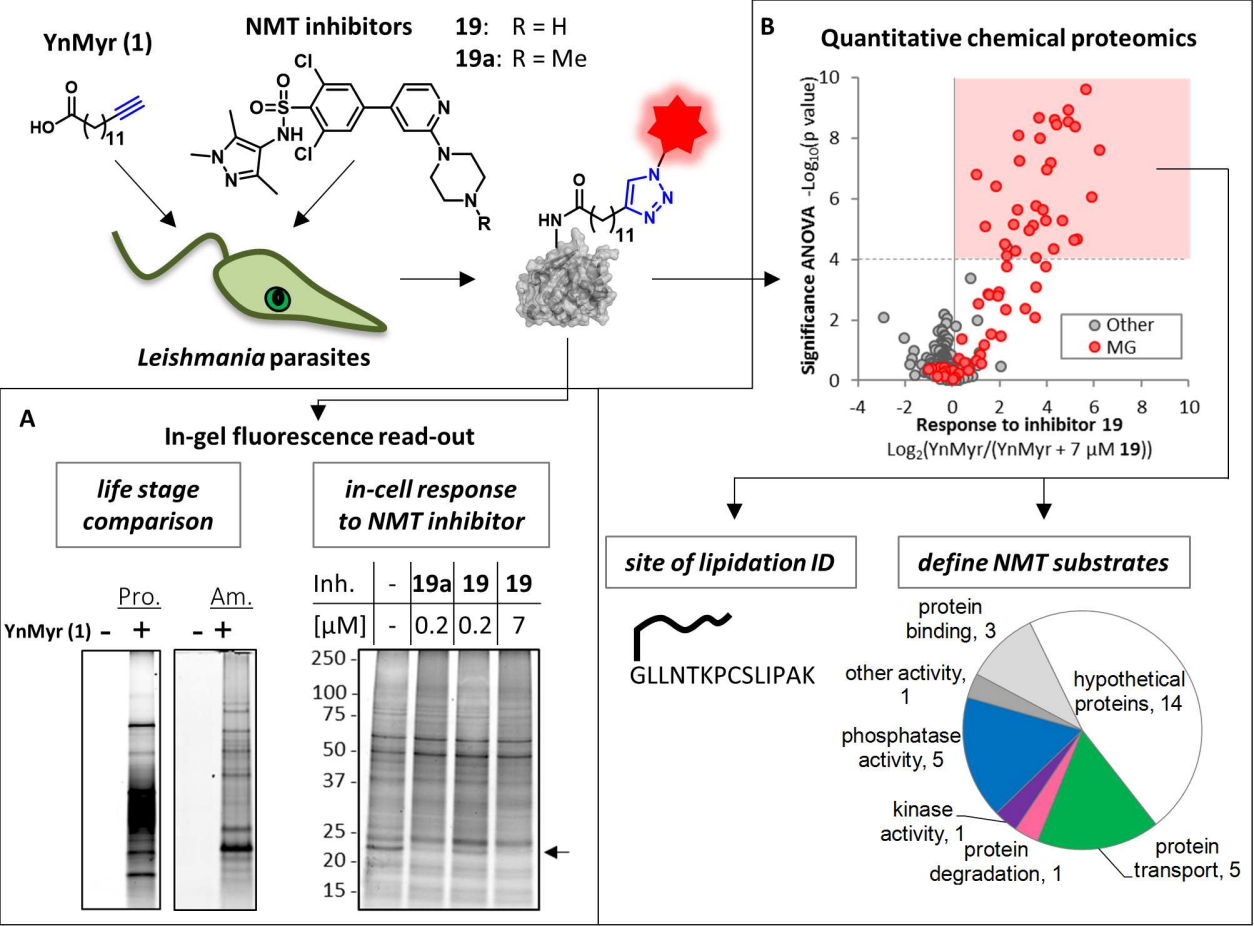
YnMyr (1)
NMT inhibitors
19: R = H
19a: R = Me
Leishmania parasites
B
Quantitative chemical proteomics
Significance ANOVA -Log10(p value)
Other
MG
Response to inhibitor 19
Log2(YnMyr/(YnMyr + 7 µM 19))
A
In-gel fluorescence read-out
life stage comparison
in-cell response to NMT inhibitor
Pro.
Am.
YnMyr (1) - + - +
Inh. - 19a 19 19
[µM] - 0.2 0.2 7
250
100
75
50
37
25
20
15
site of lipidation ID
GLLNTKPCSLIPAK
define NMT substrates
protein binding, 3
other activity, 1
hypothetical proteins, 14
phosphatase activity, 5
kinase activity, 1
protein degradation, 1
protein transport, 5

A

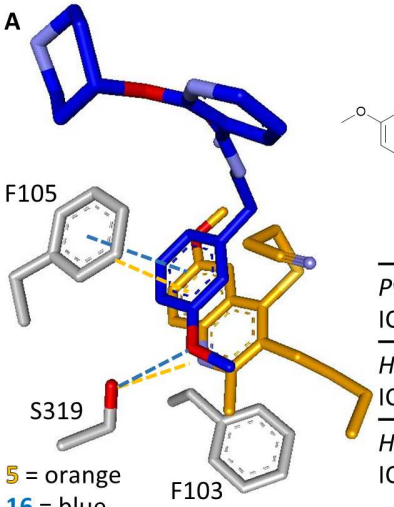

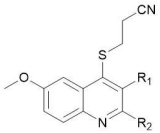

5: R_1 = *n*Bu, R_2 = Me
6: R_1 = CO_2Et, R_2 = H

	5	6	16
*Pv*NMT IC_{50} [μM]	0.027	1.73	4.74
*Hs*NMT1 IC_{50} [μM]	0.27	1.69	19.43
*Hs*NMT2 IC_{50} [μM]	n.d.	11.39	>100

B

	7	8	9
*Ld*NMT IC_{50} [μM]	0.063	0.254	0.0016
*Hs*NMT1 IC_{50} [μM]	2.1	28.5	0.027
Ld EC_{50} [μM]	>30	10-30	10-30

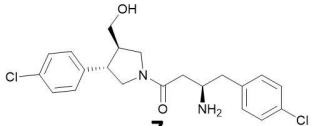

7

\+

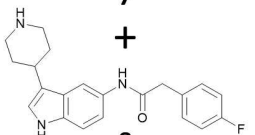

8

→

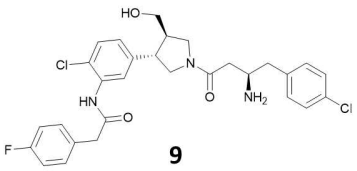

9

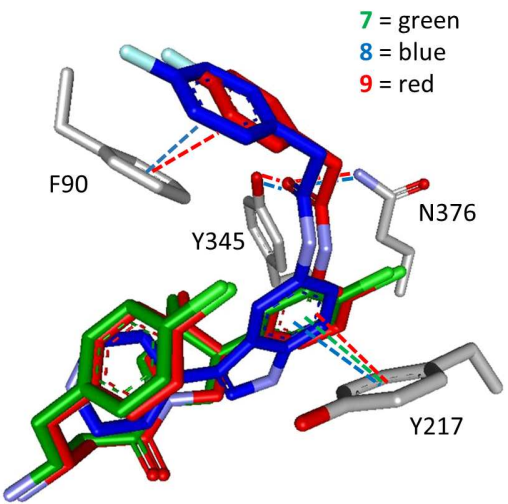

A

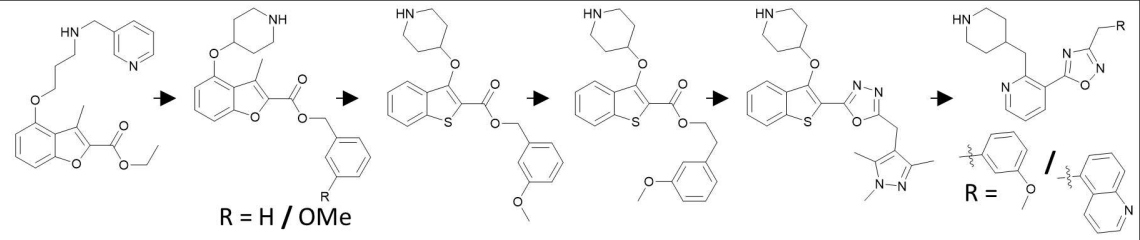

	RO-09-4609 (10)	11/12	13	14	15	16/17
*Pf*NMT IC_{50} [µM]	51	0.27 / 0.60	0.83	0.12	0.008	0.027 / 0.0017
*Hs*NMT1 IC_{50} [µM]	>1000	>100 / >200	3.2	2.2	0.06	0.27 / 0.024
Pf 3D7 EC_{50} [µM]		1.2 / n.d.	2.0	4.2	0.3	3.5 / 0.21

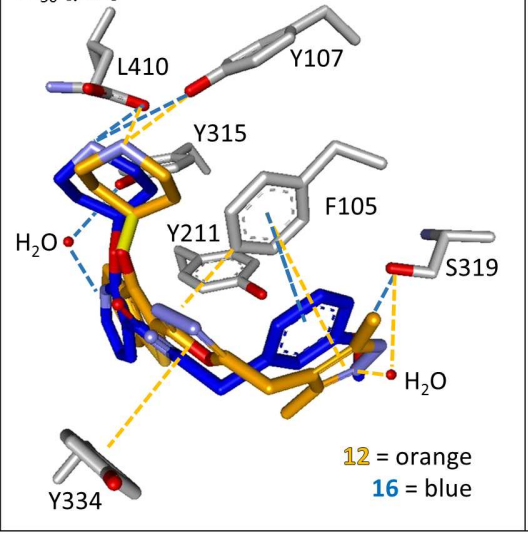

B

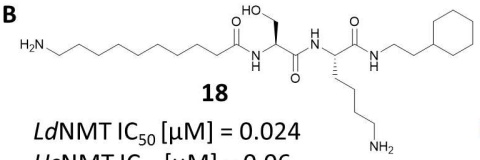

18

*Ld*NMT IC_{50} [µM] = 0.024
*Hs*NMT IC_{50} [µM] = 0.06

CoA = red
Myristic acid = blue
18 = orange

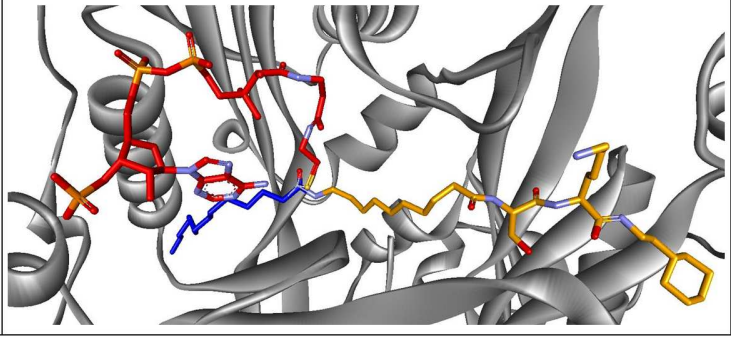

A

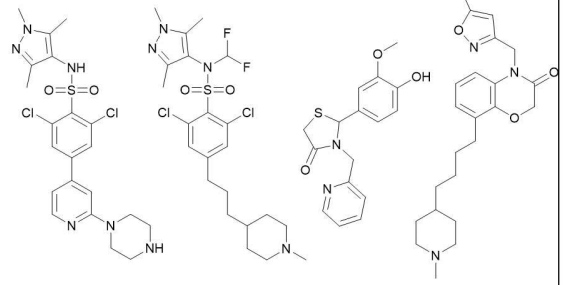

	DDD85646 (19)	20	21	22
*Tb*NMT IC_{50} [μM]	0.002	0.002	0.27	<0.002
*Hs*NMT1 IC_{50} [μM]	0.003	0.012	>100	0.04
Tb EC_{50} [μM]	0.002	0.001	14	0.007
B:B	<0.1	1.6	ND	27

B